THE EFFECT OF GRAIN SIZE ON THE YIELDING BEHAVIOR OF VERY LOW CARBON STEEL

Thesis by

Thomas L. Russell

In Partial Fulfillment of the Requirements

For the Degree of

Doctor of Philosophy

California Institute of Technology

Pasadena, California

1958

ACKNOWLEDGEMENTS

The author wishes to express his sincere appreciation to Professors Donald S. Clark and David S. Wood, who directed this research, for their aid and encouragement. The assistance of Professor Thad Vreeland, Jr., who contributed many valuable comments and suggestions during the course of this research is also acknowledged with thanks. The assistance of Mr. Kirk Irwin and Mr. Martin Conneally in specimen preparation and performance of the tests is greatly appreciated.

The author is indebted to the International Nickel Company and Shell Oil Company for fellowship grants.

The testing program was conducted under a contract with the Office of Ordnance Research, United States Army. Appreciation is extended to this agency for support of this work.

ABSTRACT

This thesis presents the results of an experimental investigation of the effect of grain size on the yielding behavior of very low-carbon steel. Steel specimens of five grain sizes were produced for testing. The average grain diameter of these specimens ranged from 1.1×10^{-3} in. to 8.1×10^{-3} in. Two types of tensile tests were performed, one by the application of very low loading rates and the other by the rapid application of a constant stress. Both types of tests were performed at temperatures of $72^{\circ}F$ and $-320^{\circ}F$, while a few rapid loading tests were performed at a temperature of $-109^{\circ}F$.

Both the static upper and lower yield points are observed to increase linearly with $d^{-1/2}$, where d equals the average grain diameter. Delay time and pre-yield microstrain for specimens that exhibited a yield point were determined from the rapid loading tests conducted at room temperature. Delay time decreases with increasing grain diameter for a given stress.

The experimental results are compared with several dislocation models for yielding. These models are shown to be incapable of describing the experimental results of this investigation. A more detailed model, based on Cottrell's yielding mechanism, is described.

Plastic deformation by twinning occurred in both static and rapid loading tests performed at a temperature of $-320^{\circ}F$. A critical stress for twinning was observed. This stress is independent of stress rate in the range from 10^{7} lb/in^{2} sec to 500 lb/in^{2} sec. The critical twinning stress increases linearly with $d^{-1/2}$. The existence of a critical stress for twinning is shown to be compatible with Cottrell and Bilby's theory for the formation of twin bands.

TABLE OF CONTENTS

LIST OF TABLES

LIST OF FIGURES

LIST OF FIGURES (Cont'd)

I. INTRODUCTION

Plastic deformation of metals has been observed and studied by numerous investigators. Many of these investigations have been concerned with understanding the initiation of plastic deformation in terms of the movement of certain types of crystal imperfections, called dislocations. Dislocations are able to move through a crystal lattice under the influence of an applied stress leaving a slipped region in their wake.

A yield point has been observed in several materials at the initiation of gross plastic deformation. The yield point is defined as the initiation of very rapid plastic deformation without any increase in the applied stress. The upper and lower yield points have been defined in order to further describe this phenomenon. The upper yield point is the stress at which large plastic strains are initiated. The lower yield point is the smallest stress required for the continuation of plastic deformation.

Steel exhibits a yield point at the onset of gross plastic deformation by slip. Because this alloy is utilized extensively in engineering applications, an understanding of its yielding behavior is of great importance.

The existence of a yield point in steel has been shown to be dependent on the presence of carbon and nitrogen as an interstitial solute atom in the α-iron crystal lattice (1), (2). Holden and Hollomon (3) have reported that a yield point is not present when large single crystals of iron containing carbon and nitrogen are subjected to stress levels

which cause slip. Consequently the phenomenon of a distinct yield point in steel must be associated with: 1) the presence of a sufficient amount of carbon and/or nitrogen; and 2) the presence of grain boundaries.

Wood and Clark (2), (4), (5) have shown that there is a definite period of time before the initiation of yielding in annealed low carbon steel, when a specimen is subjected to a rapidly applied constant stress. The time period from loading until yielding occurs, during which the material is held at a constant stress, has been named the delay time. The occurrence of a small amount of plastic deformation before yielding has been reported by several investigators (6), (7). This small pre-yield plastic strain has been labeled microstrain.

Several theoretical models have been proposed to quantitatively describe the delay time for yielding in low carbon steel (8), (9), (10). All of these models are descriptions of a basic mechanism which involves the following three concepts: 1) the thermally activated release of a dislocation from a carbon and/or nitrogen atmosphere, as suggested by Cottrell and Bilby (11); 2) the generation of dislocations by a Frank-Read source (12); 3) the restriction placed on dislocation motion by grain boundaries, as suggested by Cottrell (13).

Interstitial impurity atoms diffuse to dislocations and form atmospheres around the dislocations. The elastic strain energy of the crystal is decreased by the diffusion of interstitial atoms to dislocations. An atmosphere therefore acts as a barrier to dislocation motion because the combined elastic strain energy of dislocation and impurities is in-

creased as a dislocation and its atmosphere are separated. Thus the applied stress required to liberate a dislocation from its atmosphere is considerably larger than the stress required to move a free dislocation in a lattice. Cottrell and Bilby (11) have suggested that a dislocation escapes from an atmosphere if the local stress acting on a segment of the dislocation is increased to a value greater than the applied stress by a thermal fluctuation of the crystal lattice. A dislocation once liberated from its atmosphere is free to move, under the action of the applied stress.

A multiplication process for slow-moving dislocations has been proposed by Frank and Read (12). This process essentially constitutes a dislocation source, thereby suggesting the generation of a large number of dislocations at some position in the crystal lattice.

The dislocations generated by a Frank-Read source move outward under the action of an applied stress until encountering an obstacle, such as a grain boundary, which blocks further motion. Hence, as dislocations are generated, they tend to pile up at a grain boundary. Cottrell (13) has proposed that yielding will occur when the resistance offered by the grain boundary to the movement of dislocations is overcome. According to Cottrell, when a sufficient number of dislocations have piled up at a grain boundary, slip is produced in the next grain and thereby catastropic slip is initiated in successive grains. This catastropic slip across grains produces the rapid increase in strain associated with the yield point. The delay time in rapid loading experiments can be associated with the time for generation of the necessary number of dislocations, which when piled up at the grain boundary, will

produce slip in the adjacent grain. The observed microstrain is associated with dislocation generation and movement within single grains before yielding occurs.

Fisher (8), Vreeland and Wood (9), and Cottrell (10) have calculated expressions for the delay time as a function of stress and temperature which agree with the experimental data of Wood and Clark (4), (5). Each of these treatments involve the same general dislocation mechanism as previously outlined. However, slightly different conditions for dislocation generation and for the initiation of slip at a grain boundary were considered in each treatment.

The delay time given by Fisher's and Cottrell's expressions is independent of the grain size of the material tested. Although Vreeland and Wood's expression for delay time is a function of grain size, the term involving the grain diameter is only a second order correction term. Consequently all of these expressions give a delay time that is essentially independent of grain size.

Fisher's and Cottrell's treatment predict that the static yield point should also be independent of grain size. However, this is in sharp disagreement with experimental results of several investigations (14), (15), (16). These investigations have shown that the lower yield point increases linearly with increasing values of $d^{-1/2}$, where d is the average grain diameter. Vreeland and Wood's treatment of the yielding process predicts that the static yield point should be an increasing linear function of $d^{-1/2}$.

According to Vreeland and Wood's calculation of delay time, a plot of the log of delay time, as a function of stress for different grain

sizes, should be of the form shown in figure 1.

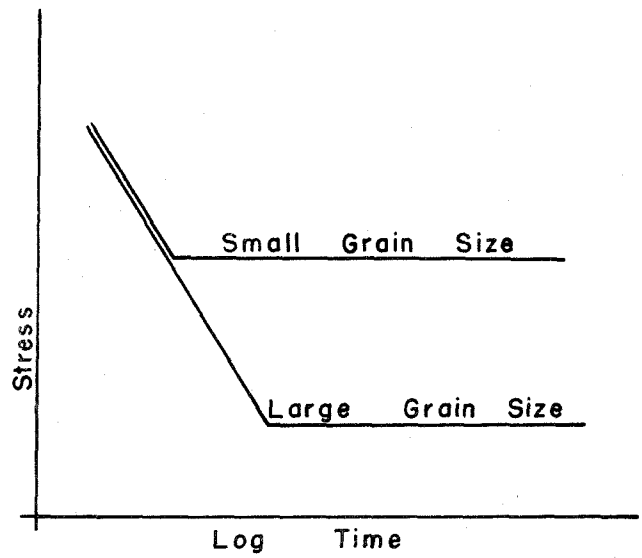

Fig. 1 Delay Time as a Function of Stress and Grain Size as Predicted by Vreeland and Wood's Treatment of Yielding.

All of the calculations of delay time have been based on the fact that only one dislocation is generated per thermal fluctuation at a Frank-Read source. However, a closer examination of the generation process results in the conclusion that a burst of many dislocations would most likely result from one thermal fluctuation. An estimate of the number of dislocations in a burst has been made by Fisher, Hart and Pry (17).

Another problem resulting from Fisher's and Vreeland and Wood's treatments involves the ratio of the binding energy between a dislocation and its atmosphere to the energy of a free dislocation. This ratio, obtained by fitting either expression for delay time to the experimental data of Wood and Clark (4), (5), is approximately 30 times smaller than

values obtained from other considerations. Cottrell's treatment does not directly involve this difference and therefore would seem to be an improvement. However, his treatment is a little more vague, in that the details of the process are not as well defined.

In spite of the shortcomings of these analytical treatments of yielding behavior, there is considerable evidence to support the general yielding mechanism originally proposed by Cottrell. However, the details of this mechanism are certainly not well defined by the existing models for yielding.

The purpose of the present investigation is to study the effect of grain size on the yielding behavior of a low-carbon steel in order to establish a more detailed model for yielding. The experimental techniques to be used in this investigation include both static and rapid loading tests of a series of low-carbon steel specimens of various grain sizes. The static tests will determine both the upper and lower yield points as a function of grain size. The rapid loading tests will establish the relationship of delay time and microstrain at yielding to the grain size of the steel.

This investigation will include tests at various temperatures, since the influence of temperature is certainly important in a thermally activated process.

The existing models for yielding will be examined to determine which are compatible with the experimental results of this investigation. If the existing models for yielding do not satisfactorily account for the experimental results of this investigation, then possible modifications, or the possibility of a different model will be explored.

II. MATERIAL AND SPECIMEN PREPARATION

Material

The specimens used in this investigation were fabricated from 1 x 1/4 inch hot-rolled bars of a single billet from heat No. 47484 from the Torrance works, Columbia-Geneva Steel Division, United States Steel Corporation. Analysis of the heat made by the mill was given as the following:

Carbon	0.09%
Manganese	0.30%
Phosphorus	0.020%
Sulfur	0.037%

All specimens were decarburized by treatment in wet hydrogen and then were given a slight recarburization. The purpose of the decarburization was to remove all iron-carbide particles. The small amount of carbon added after decarburization was sufficient to produce the yielding behavior typical of carbon steels, but not sufficient to produce microscopically visible carbide particles in the structure. A typical microstructure is shown in figure 2.

Grain Sizes

A variation in the grain size of the low-carbon steel used in this investigation was produced by two techniques: 1) By annealing the material at suitable austenitizing temperatures; 2) By the recrystallization of previously cold worked material at temperatures below the transformation temperature. The size of ferrite grains, which result from annealing, increase as the temperature in the austenitic range to which the steel is heated is increased. Austenitic grain size increases with

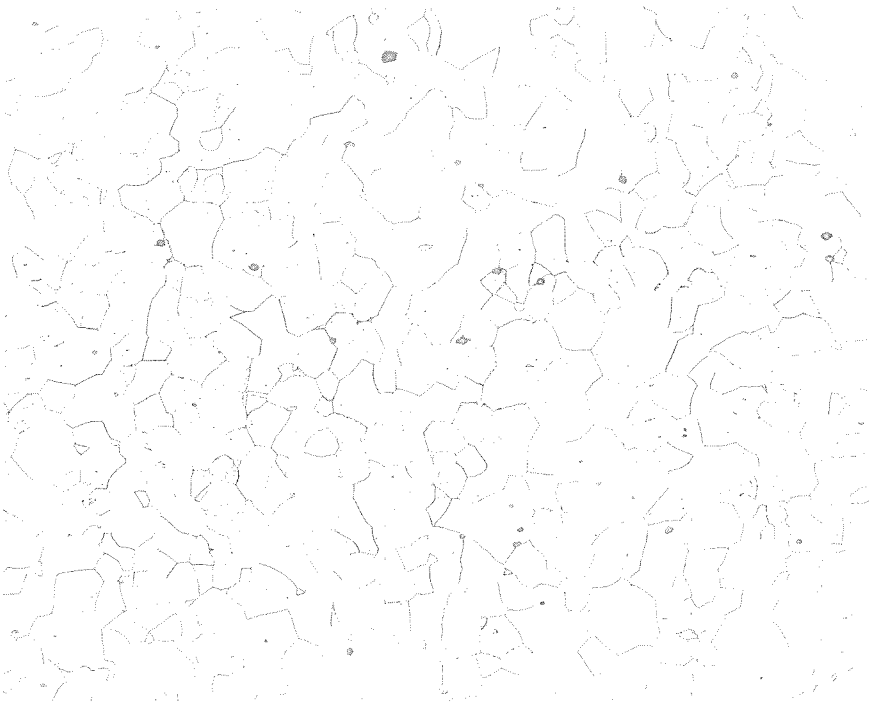

Fig. 2 Typical Microstructure, Annealed at 1660°F, Decarburized and Recarburized. 150X.

temperature and upon cooling the ferritic grain size reflects this increase.

Recrystallized structures result from plastically deforming the steel, then heating it to a temperature below the phase transformation temperature and holding for a period of time. The size of the recrystallized grain structure is a function of the amount of plastic deformation. There is a critical value of plastic strain which must be exceeded in order to produce recrystallization, for a given time at a given temperature. The recrystallized grain size is a maximum when the metal has been subjected to this critical value of strain. The resulting grain size decreases with increasing amounts of plastic deformation.

For the purposes of this investigation, the grain size is reported in terms of the average grain diameter, which is equal to the square root of the average grain area observed on a plane intersecting the specimen. This value of the average grain diameter does not necessarily represent the true value of the grain size. Several factors exist which tend to confuse the interpretation of the average diameter. One important factor is that a grain structure in reality consists of grains of different sizes and therefore the distribution of the grain size should be considered. A second factor involves the question of how the average diameter of grains delineated on a plane section is related to the average volumetric diameter of the grains. In addition, the diameter is only an approximate dimension since grains are not regular polyhdra but are of an irregular shape. After a study of these and other considerations, which are outlined in Appendix A, the average grain diameter on a plane was chosen to represent grain size.

The grain size produced by recrystallization was determined for the steel used in this investigation as a function of the amount of plastic strain prior to heat treatment. This information is plotted in figure 3, for a temperature of approximately 1250°F and for a time of approximately 2 hours at temperature. Values of 8, 9, 11, and 18 per cent strain were chosen to obtain four of the grain sizes used in this investigation. Two additional grain sizes were produced for study by annealing at 1660 and 2400°F.

The average grain area for a particular treatment was determined by counting the number of grains in a given area of one or two photomicrographs of a specimen. The average was then taken for as many as ten specimens which had received the same treatment. The total number of grains counted was between 2000 and 4000 for each grain size. The average diameter was taken as the square root of this average size. The resulting average grain sizes are given in table I.

Typical distribution curves of grain diameters for specimens that have been strained 8 and 9 per cent, plotted in figure A-2 of Appendix A, indicate that the distributions are approximately the same for these two structures. This observation would lead one to expect that the specimens of these grain sizes would exhibit very similar mechanical properties. This was observed to be the case in tests performed during this investigation. Therefore the specimens with average grain diameters equal to 8.7 and 7.3×10^{-3} in. are considered as the same grain size, with an average grain area and average grain diameter of 65×10^{-6} in.^{2} and 8.1×10^{-3} in. respectively.

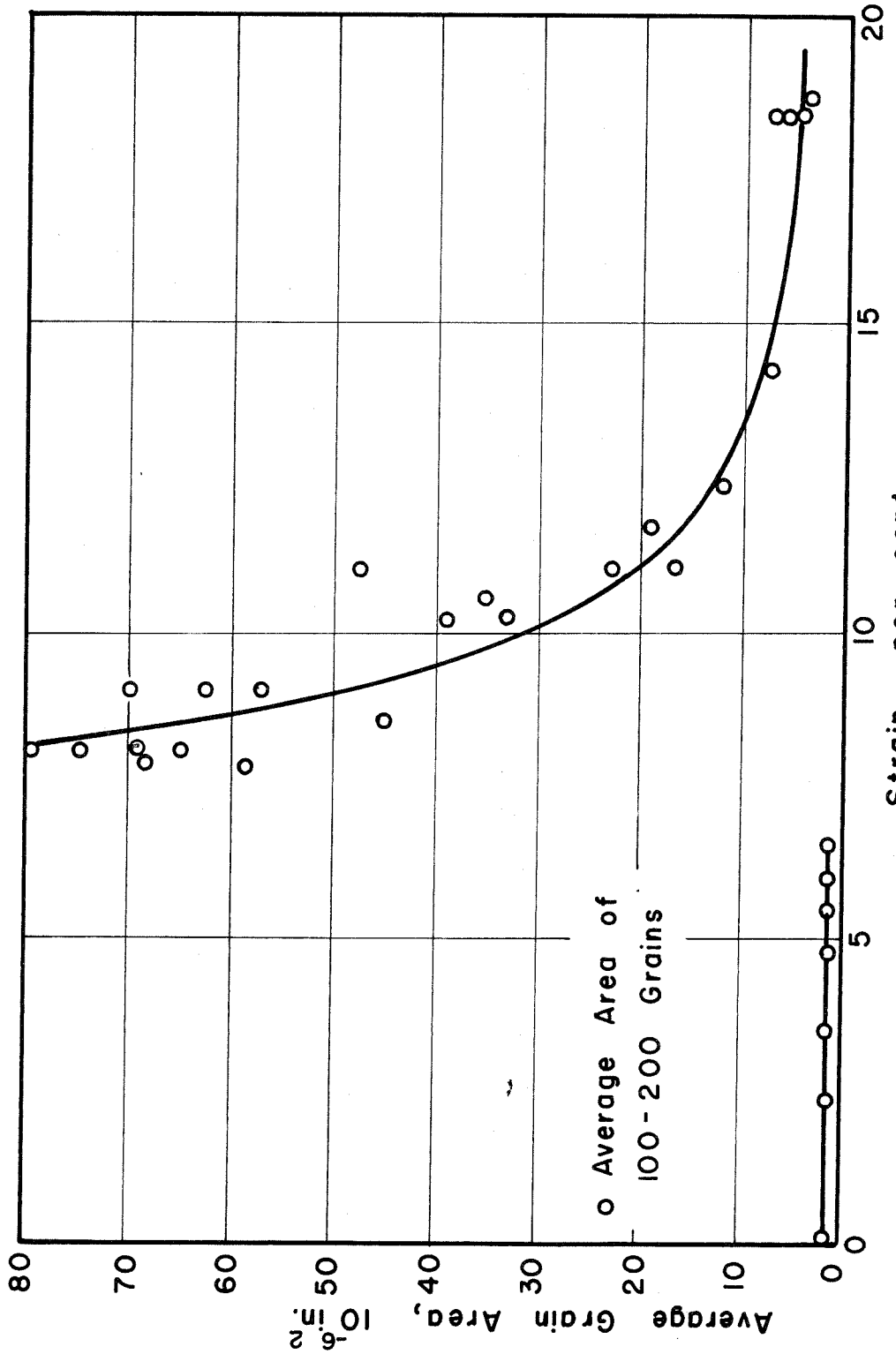

Fig. 3 Recrystallized Grain Diameter vs. Per Cent Cold Work.

TABLE I

AVERAGE GRAIN SIZES OF THE TEST SPECIMENS

Treatment	Average Area 10^{-6} in.^{2}	Average Diameter* 10^{-3} in.
Strained 8% and recrystallized	76.5	8.74
Strained 9% and recrystallized	53.8	7.33
Strained 11% and recrystallized	30.7	5.54
Annealed at 2400° F	18.8	4.33
Strained 18% and recrystallized	6.00	2.45
Annealed at 1650° F	1.25	1.12

*Average Diameter = $\sqrt{\text{Average Area}}$

The comparison of experimental results with theoretical considerations would be facilitated if the grain sizes produced for this investigation were uniform. A study of the different grain sizes produced by both annealing and recrystallization indicated that these grain structures were not uniform. The results of this study are presented in Appendix A. Several attempts were made to produce more uniform grain sizes by various heat treatments, but without success. This work is also reported in Appendix A. The diameter of the largest grains observed in each of the five grain sizes was approximately three times the average value.

Specimen Preparation

Three types of specimens were used in the course of this investigation. These are shown in figures 4, 5, and 6. The specimens shown in figures 4 and 5 were used for testing the recrystallized material. The specimen shown in figure 4 is the one used in the majority of the tests. Only a few specimens of the type shown in figure 5 were tested. These larger specimens were used to determine the influence of specimen dimensions on the experimental results. The specimen shown in figure 6 was employed in tests on the annealed material.

The specimens shown in figure 4 and 6 were fabricated by different processes because of the differences in fabrication techniques that are required in producing specimens of annealed and recrystallized material. The specimens to be annealed could be formed by the customary machining or cold forming methods because the annealing treatment was the last operation and therefore any residual stresses were completely removed.

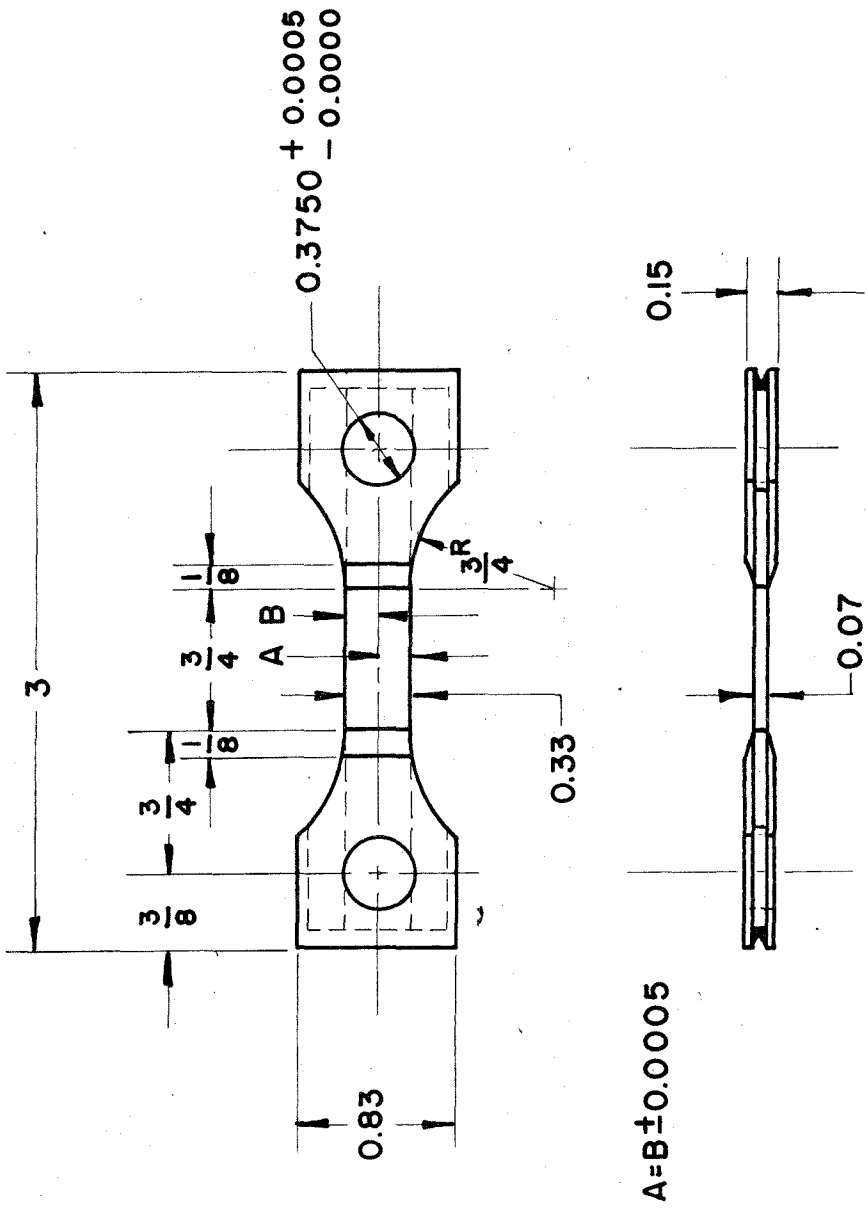

Fig. 4 Test Specimen for Recrystallized Material.

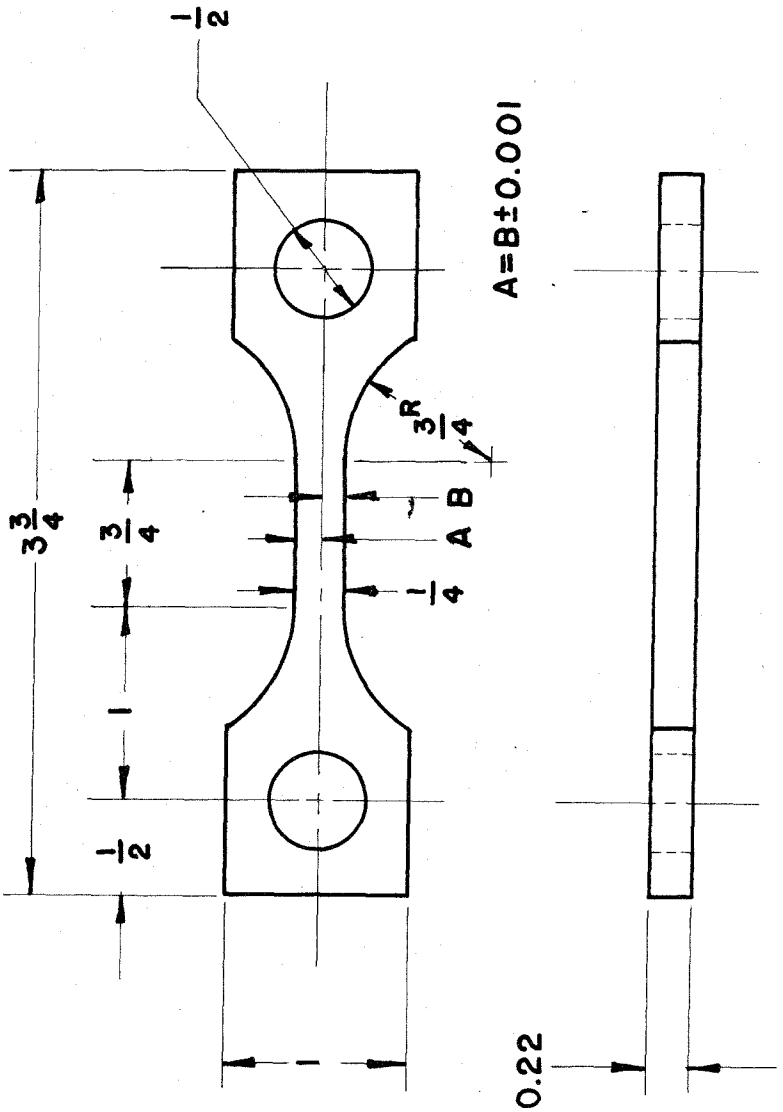

Fig. 5 Special Large Test Specimen for Recrystallized Material.

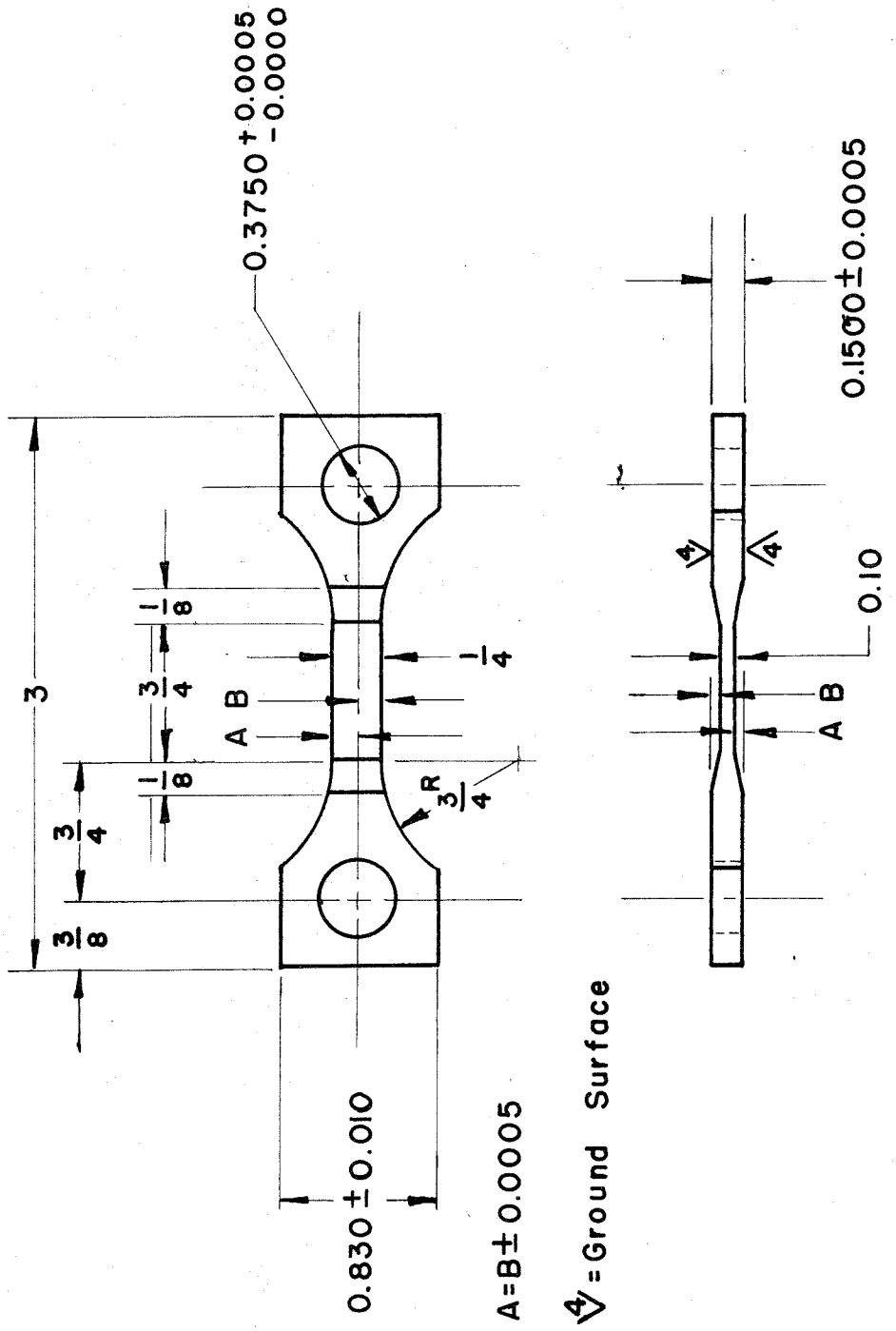

Fig. 6 Test Specimen for Annealed Material.

In the case of the recrystallized specimens, the steel must be strained before any machining operations can be performed to reduce the area of the gage section. Consequently, stresses introduced by machinig operations would affect the resulting grain size. If the material was recrystallized before machining, residual stresses would be introduced. The design shown in figure 4 was such that no machining operations on the gage section were performed after recrystallization, and therefore the possibility of damage to the rather thin gage section was decreased.

The procedure followed in producing the small specimens of recrystallized steel, shown in figure 4, is summarized in the following outline:

1) The hot rolled bar stock, 1/4 in. by 1 in., was cut into short lengths and finish ground on two surfaces.
2) The ground bars were cold rolled into strips 40 in. long, 1 in. wide, and 0.07 in. thick.
3) Gage lengths 0.35 in. wide by 27 in. long by 0.07 in. thick, were machined into the strips.
4) The strips were annealed at 1670° F for 1 hr and 20 min in a hydrogen atmosphere.
5) The strips were strained in a hydraulic Olsen Universal Testing Machine. The strain was measured between two points in the gage length 18 in. apart. The strain measurements were made by means of a scale with a least reading of 0.01 in. Several strips were plastically strained 8, 9, 11 and 18 per cent.

6) The strips were recrystallized at 1270 ± 20° F for 24 hrs in a hydrogen atmosphere.

7) The gage length of the long strips were cut into short lengths, 2-7/8 in. long, to be used as gage sections for the specimens.

8) The gage sections were decarburized by heating to 1220 ± 20° F for 72 hrs in a wet hydrogen atmosphere.

9) The gage sections were recarburized at 1220 ± 20° F for 1 hr in a hydrogen atmosphere containing n-heptane.

10) The gage sections were given a homogenizing treatment at 1220 ± 20° F for 6 hrs in a helium atmosphere. This treatment was employed in order to decrease any existing carbon concentrate gradients.

11) The gage sections were assembled with the end parts and the assembly was held together by a small machine screw. A silver solder wire was inserted around the groove on three sides of the end assembly.

12) The silver soldering was accomplished by heating the complete assembly to approximately 1220° F for 1/2 hr in a purified hydrogen atmosphere, and then furnace cooling.

13) The 3/8 in. diameter holes at each end were machined with the aid of an alignment jig. This process also cut away the machine screw originally used to hold the assembly together during silver soldering.

The procedure followed in producing the large specimens of recrystallized steel, shown in figure 5, is summarized in the following outline:

1) The hot rolled stock was cut into 24 in. lengths and finish ground on two surfaces. The final dimensions were 0.22 in. by 1 in. by 24 in. long.

2) The bars were strained in a hydraulic Olsen Universal Testing Machine. The strain was measured between two points 10 in. apart. The strain measurements were made by means of a scale with a least reading of 0.01 in. Several bars were strained 8 per cent.

3) The bars were cut into sections and machined into specimens of the type shown in figure 5.

4) The specimens were recrystallized and decarburized by heating to 1240 ± 30° F for 292 hrs in a wet hydrogen atmosphere.

5) The specimens were recarburized at 1240 ± 20° F for 3.5 hrs in a hydrogen atmosphere containing n-heptane.

6) The specimens were given a homogenizing treatment for 10 hrs at 1240 ± 20° F in a helium atmosphere.

The procedure followed in producing specimens of annealed steel, shown in figure 6, is summarized in the following outline:

1) The hot rolled stock was cut into short lengths and finish ground on four sides. The specimen blank dimensions were 0.150 in. by 1 in. by 3 in.

2) The thickness of the gage section was reduced from 0.150 in. to 0.10 in. by coining in a die specially constructed for this purpose.

3) The blank was finish machined to the shape shown in figure 6.

4) One group of specimen was annealed at 1600 ± 20° F for 2 hrs. Another group was annealed at approximately 2400° F for 2 hrs. Both groups were annealed in a hydrogen atmosphere.

5) The specimens were decarburized in a wet hydrogen atmosphere. The specimens annealed at 1600° F were decarburized 75 hrs at 1230 ± 40° F, while those annealed at 2400° F were decarburized for 70 hrs at 1240 ± 20° F.

6) All the specimens were recarburized for 1 hr at 1220 ± 20° F in a hydrogen atmosphere containing n-heptane.

7) The specimens were given a homogenizing treatment for 4 hrs at 1220 ± 20° F in a helium atmosphere.

The hydrogen and helium atmospheres, referred to in the above descriptions of the preparation of specimens, was the usual commercial grade of gas which was passed through the following equipment before entering the furnace muffle:

1. "De-oxo" catalytic hydrogen purifier.
2. Drying tower containing $CaCl_2$.

The purified hydrogen atmosphere referred to above was produced by passing gas through the following equipment:

1. "De-oxo" catalytic hydrogen purifier.
2. Drying tower containing $CaCl_2$.
3. Activated charcoal trap at liquid nitrogen temperature.
4. Electric furnace containing sponge titanium at 1600° F.

The wet hydrogen atmosphere was obtained by bubbling commercial grade hydrogen through water maintained at a temperature of approximately 150° F, before it entered the furnace muffle. The recar-

burizing hydrogen atmosphere was the result of bubbling hydrogen through n-heptane at room temperature, approximately 75° F, before it entered the furnace.

III. EQUIPMENT

Static Loading Test Equipment

The static tests at room temperature were performed in two testing machines:

1) An Olsen Universal Testing Machine, using the 0-15,000 lb range with a least reading of 1 lb.
2) An Instron Universal Testing Machine, using successive ranges of 0-100, 0-200, 0-500, and 0-1000 lbs with least readings of 0.5, 1, 2.5, and 5 lbs respectively.

Both machines utilized a screw drive for cross-head motion. The moving and stationary head of both testing machines were linked to the specimen by means of short lengths of chain in order to reduce bending stresses in the specimen.

Strain in the gage section of the specimens was determined with Baldwin A-7 or A-18 SR-4 resistance sensitive wire strain gages. A gage was bonded to each side of the specimen with duco cement, after the surfaces had been roughened with 000 emery paper. The gages were applied and dried in the manner suggested by the manufacturer.

The strain gages on the specimens tested in the Olsen Testing Machine were electrically connected into a Wheatstone bridge circuit containing two temperature compensating gages and a decade resistance box. The bridge was energized by a dry cell battery. Resistance changes in the active legs were balanced by adjustment of the variable resistance in one dummy leg. The bridge balance was indicated by a galvanometer connected across the bridge. The strain sensitivity of this measuring system is approximately 5×10^{-6} in./in. Large strains

were measured after gage failure by means of the average readings of two dial gages which measured the relative motion of the specimen grips.

The tests performed in the Instron Testing Machine were made with the two active gages electrically connected into a bridge with two temperature compensating gages. The bridge was directly connected to a Baldwin SR-4 Strain Indicator, thereby allowing the strain values to be read directly. The strain sensitivity of this system was approximately 2×10^{-6} in./in. There was no perceptible difference in the results of tests performed in the two testing machines.

The bending stresses in the first few tests were measured during the course of the static tests by switching the electrical connections during the test so that the signals of the two active gages are subtracted. When the gages are connected in this manner the output signal of the bridge is proportional to the bending stress in the specimen. Bending stresses were measured in later tests by connecting the gages to measure bending and then loading the specimen to stresses well within the proportional limit of the specimen. If the bending stress was small the gages were reconnected into the regular circuit and the static test was performed. A small preload was maintained on the specimen after the bending measurements in order to prevent the occurrence of any additional misalignments. In all cases, the measured bending stress was less than 5 per cent of the tensile stress in the specimen.

Rapid Load Testing Equipment

The equipment employed in the rapid loading tests at room temperature and all tests at low temperatures, was specially constructed

for this investigation. This equipment consists of three parts: 1) A rapid load testing machine; 2) A control system; 3) A recording system. The design and construction of this equipment has been completely described in a special report (18). The rapid load testing machine is a pneumatic-hydraulically operated mechanism designed to rapidly apply a constant tensile force to a specimen in order to permit the determination of the deformation in the specimen as a function of time. The control system consists of the proper hydraulic and pneumatic control equipment to supply and regulate the pressures required at the rapid load testing machine. The recording system includes a recording oscillograph, amplifiers and power supplies. The recording system records the electrical signal from two resistance sensitive wire strain gage bridges which are used to measure load acting on the specimen and strain in the specimen. A general view of this equipment is shown in figure 7. The recording system is at the left, the rapid load testing machine is in the center, and the control system is at the right.

The rapid load testing machine, which is shown in figure 8, applies a predetermined load to a tensile specimen, causing the stress in the specimen to increase to within a few per cent of its final constant value in a period of the order of 2 or 3 x 10^{-3} sec. The maximum load that can be applied to a specimen is 2000 lb. The specimen is short enough and the rate of the rise of stress low enough that the stress may be considered to be substantially uniform throughout the gage section of the specimen at any given instant.

A schematic drawing of the rapid load testing machine is shown in figure 9. The machine applies a given load to the specimen (A) by

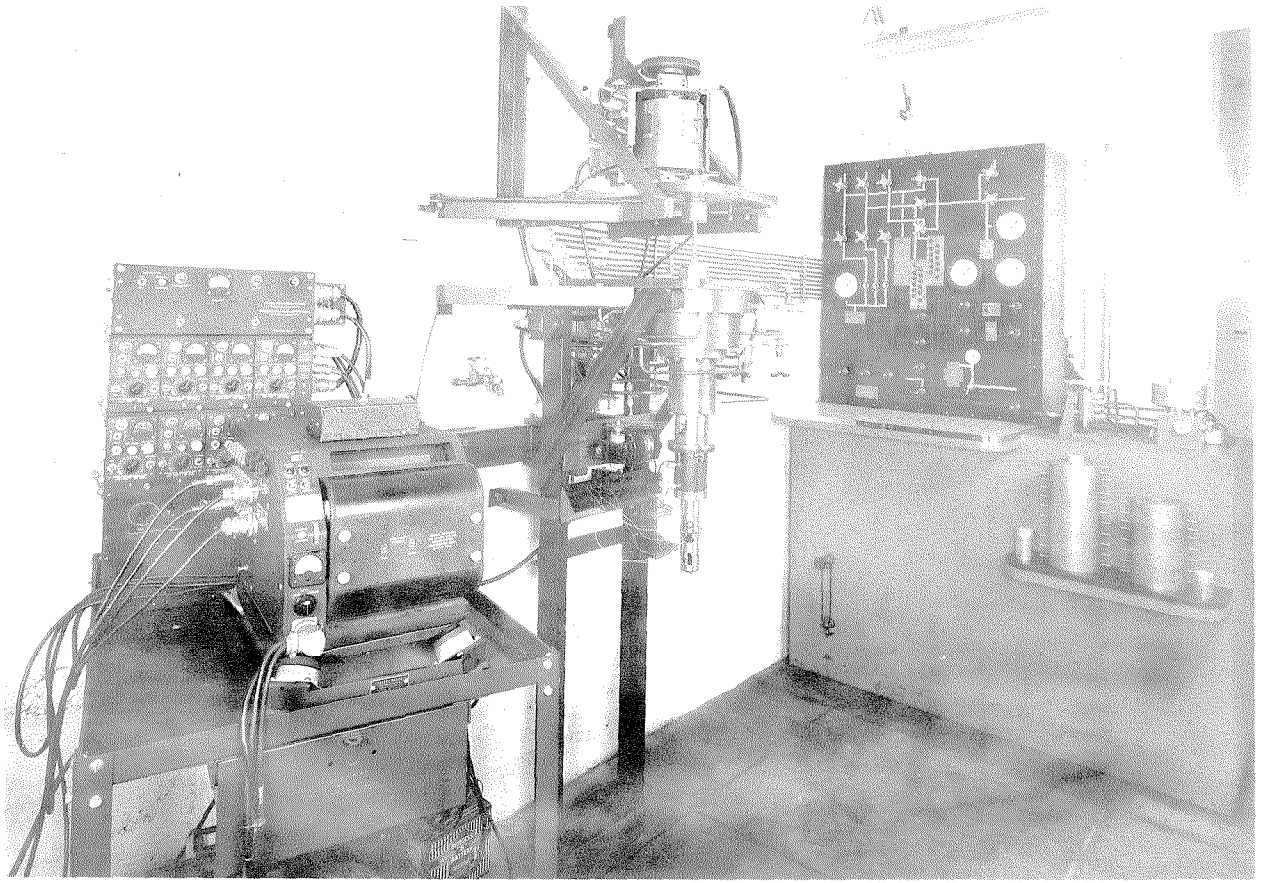

Fig. 7 General View of Rapid Load Testing Equipment.

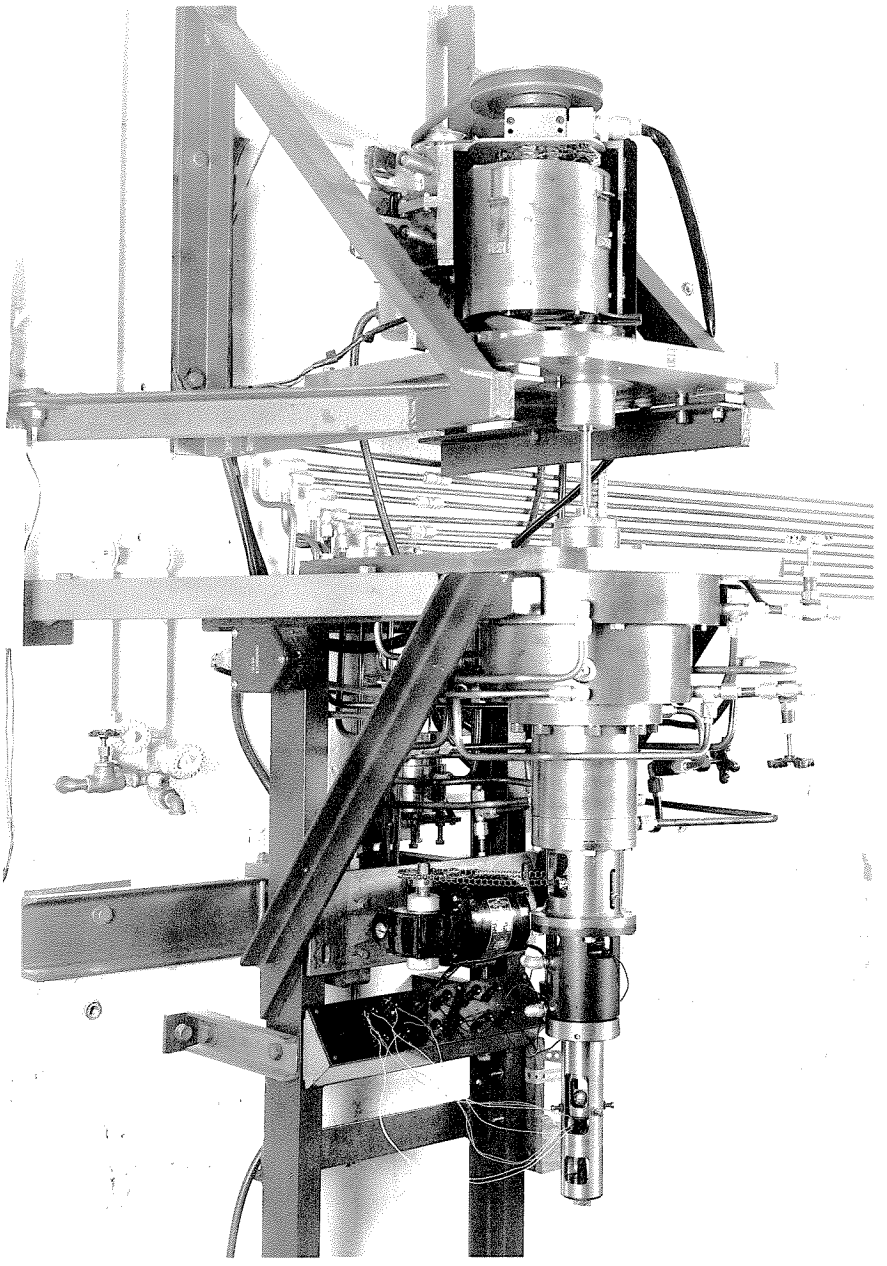

Fig. 8 Rapid Load Testing Machine.

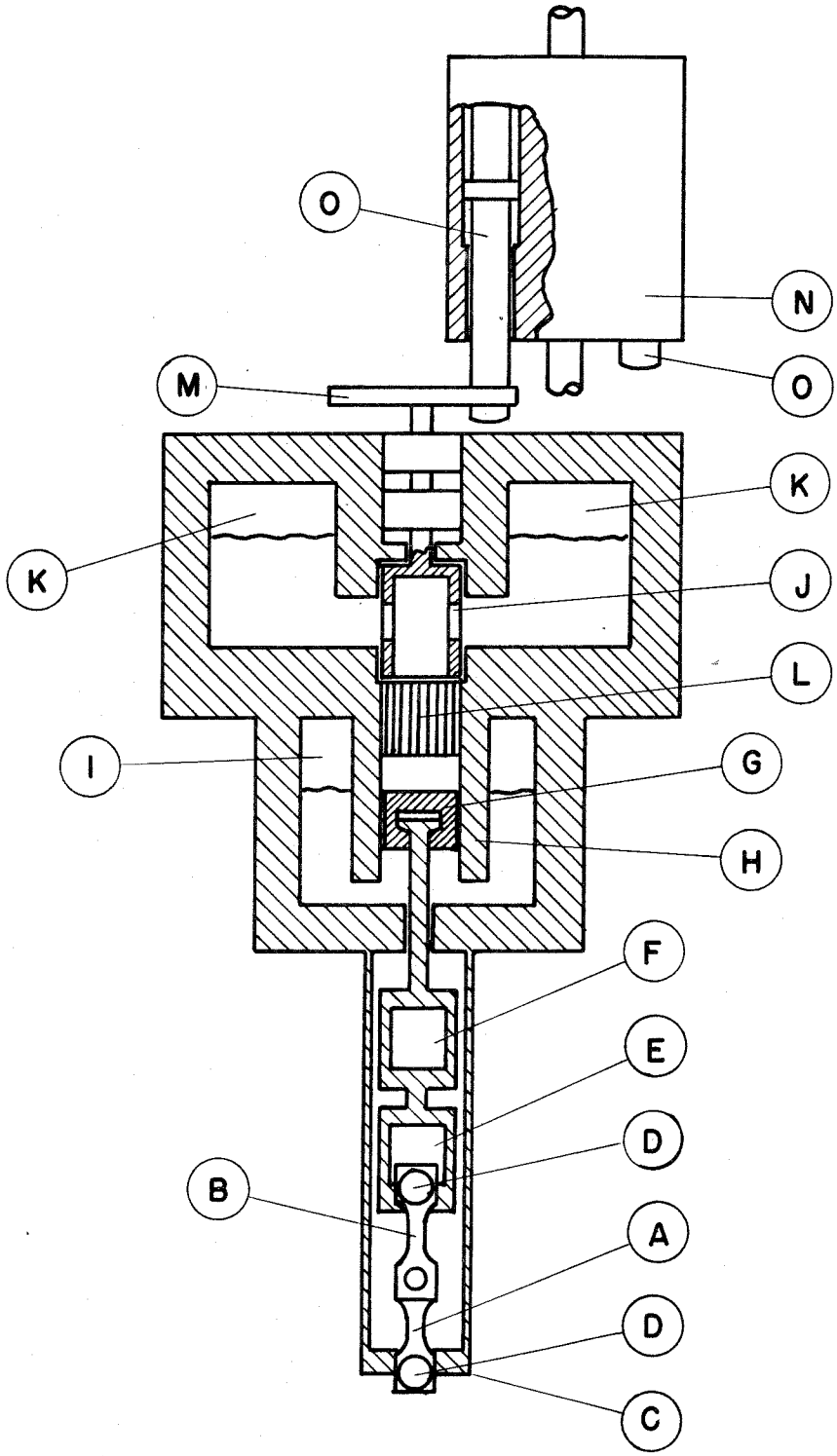

Fig. 9 Schematic Drawing of Rapid Load Testing Machine.

means of a pressure difference across the loading piston (G). The specimen (A) is connected to a stationary head (C) and through a strain bar (B) to a moving head (E). Two hardened steel spherical seats (D) are incorporated in the moving and stationary heads in order to minimize bending stresses in the specimen. The moving head (E) is joined to a dynamometer (F) which is used to measure the force applied to the specimen. The upper end of the dynamometer is in turn connected to a loading piston (G). The dynamometer is basically a thin walled circular cylinder machined from alloy steel and heat treated to impart a high elastic limit. Four resistance sensitive wire strain gages are bonded to the outer surface of the dynamometer in order to produce a signal that is proportional to the longitudinal strain in the cylinder, and hence is proportional to the stress in the specimen. The piston rod linking the dynamometer and loading piston is connected to the piston through a hardened steel spherical seat integrated into the piston body.

The piston moves in a cylinder (H). The lower side of the piston is continuously subjected to the fluid pressure in the lower pressure chamber (I). The upper side of the piston is subjected to fluid pressure which can have one of two values depending on the position of a rotary valve (J). When the valve is in the position shown in figure 9 it opens two diametrically opposite high pressure chambers (K) to the piston cylinder. When the valve is rotated one quarter revolution the cylinder is open to two chambers which are held at atmospheric pressure (not shown in figure 9).

The load is rapidly applied to the specimen by sudden rotation of

the valve, thereby subjecting the piston to only the pressure in the lower chamber. The specimen may be unloaded by again rotating the valve to the high pressure chambers. A preload may be applied to the specimen before rapid loading, when the valve is open to the high pressure chambers. The desired preload is obtained by adjusting the pressures in the upper and lower pressure chambers to impart the desired upward force to the piston.

A displacement of the piston forces fluid to flow through a cluster of small tubes (L) placed above the cylinder. The pressure drop across these tubes is proportional to the fluid velocity. Hence, due to piston motion, a viscous damping force acts on the system during the loading or unloading of the specimen.

A volume of gas is retained in each pressure chamber of the rapid load testing machine. The gas volume in the machine chambers insures an approximately constant pressure when small amounts of fluid are displaced by motion of the piston. High pressure fluid is bled in or out of the machine chambers to compensate for pressure changes due to leaks or large displacements of the piston.

The rotary valve must be rotated in steps of one quarter of a revolution in order to load and unload the specimen. This motion is achieved by rotation of a four slot geneva wheel (M) which is linked to the valve by a series of shafts. A heavy rotor (N) above the geneva wheel rotates continuously during a test. The rotor contains four pins (O) which can be forced downward so that a pin will protrude from the bottom of the rotor. When a pin is in its down position, it will engage the geneva wheel and force it to rotate one quarter of a revolution.

This action of the geneva wheel produces a 90 degree rotation of the valve. After a pin has rotated the geneva wheel it is forced up into the rotor by a ramp arrangement and latched in its up position. Each of the four pins can be unlatched individually by a cam mechanism which is energized by an electrical solenoid system. Each pin can be unlatched after any given number of rotor revolutions. Therefore, a continuous cycle of loading and unloading may be obtained in which the loaded or unloaded time is a multiple of the time for a quarter revolution of the rotor. In this investigation multiple loading cycles were not used. The load was applied and remained constant until the completion of the test and then the specimen was unloaded.

The stress vs. time relationship in the specimen during loading varied somewhat from test to test. However, a majority of the rapid loading tests were performed under loading conditions similar to those indicated by the records shown in figure 10. The stress attained approximately 98 per cent of its final value in a time of 10×10^{-3} sec after the initiation of loading in both cases shown in figure 10 and continued to increase to the final value within 0.1 sec after loading. Over time periods of several minutes there was a measurable variation in the value of the load. However, this slow drift was usually less than 2 per cent of the average value.

The second part of the rapid load testing equipment, namely the control system, is used to regulate, indicate, and supply the fluid and gas pressures in the machine. The control unit is also used to initially fill the machine with fluid. The components of this system include pressure gages, valves, tubing, fluid filter, high pressure fluid pump,

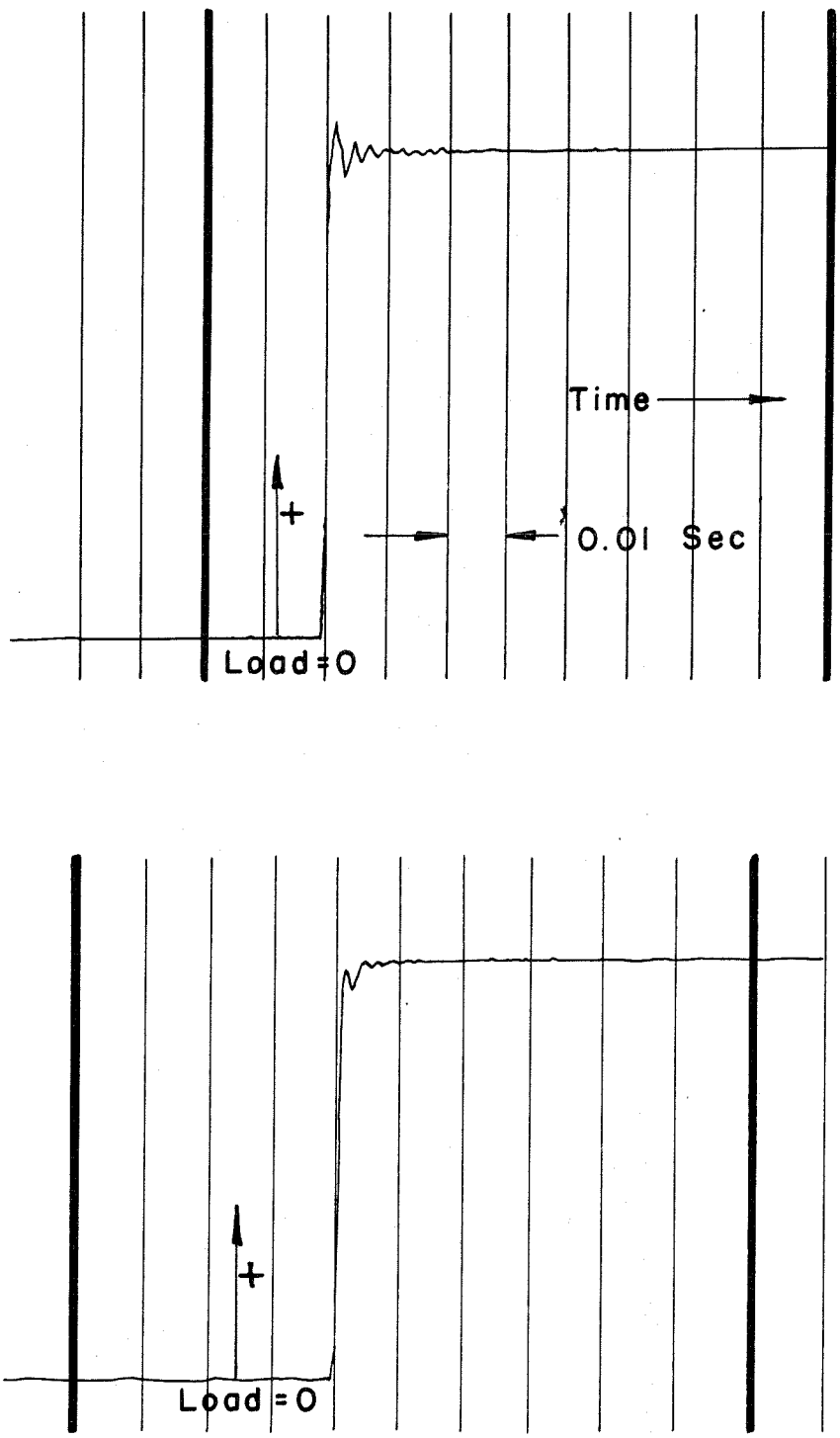

Fig. 10 Typical Rapid Loading Records.

accumulator, fluid sump, high pressure nitrogen gas cylinder and two automatic fluid pressure regulators.

Both fluid pressure regulators operate on the principle of the dead-weight pressure balance. The pistons of these regulators are made in the form of spindle valves. Any deviation of the output pressure from the value which balances the weights causes piston motion and thereby bleeds fluid in or out depending on whether the pressure has decreased or increased. One pressure regulator controls the pressure in the lower chamber of the machine. The other maintains the pressure in the upper high pressure chamber at a predetermined ratio with respect to the pressure in the lower chamber of the machine.

The recording system, which comprises the third part of the rapid load testing equipment, measures and records both stress and strain in the specimen.

The load acting on the specimen is determined by means of the dynamometer in the piston rod train of the rapid load testing machine. Four Baldwin, Type AB-4, SR-4 resistance sensitive wire strain gages are bonded with bakelite cement to the dynamometer body. Two gages are cemented with their filaments parallel to the axis of the dynamometer and two with their filaments perpendicular to the axis of the dynamometer. Each gage has a resistance of 500 ± 2.5 ohms and a gage factor of 2.5 ± 1 per cent. The gages are connected in a bridge circuit of four active legs and the bridge is connected to the recording system.

Two calibrations of the dynamometer were made by measuring change in voltage across the bridge as a function of the load on the

dynamometer. Voltage changes were measured by means of the recording system and indicated by a trace deflection on the oscillograph. In one calibration the load was measured and applied by a 150,000 lb Olsen Universal Testing Machine using the 0-15,000 lb range, with a least reading of 1 lb. A second calibration was made by hanging known dead-weights on the piston rod train and again measuring the voltage changes across the dynamometer. The weights used in this calibration provided loads ranging from 0 to 420 lbs. The weights were known to within 0.05 lb. This calibration differed by less than 2 per cent from the previous calibration.

The results of the dead weight calibration differed from the loads that are expected from the pressure regulators by no more than 1 per cent. This 1 per cent difference is within the accuracy of calculating the load from the measured diameters of the machine and pressure regulator pistons and the measured weight of the pressure regulator weights. The dead weight calibration was used for calculation of the stress in the specimen.

The strain in the specimen was measured by two Baldwin A-7, or A-18, SR-4 resistance sensitive strain gages cemented to the gage section of the specimen in the same manner as in the static tests at room temperature.

The total strain in the specimen was not recorded directly. Instead only the plastic strain in the specimen was measured and recorded. This type of measurement is accomplished by means of the strain bar which was incorporated into the piston rod train of the rapid load testing machine. The strain bar is a hardened alloy steel specimen

that is connected in series with the specimen and hence subjected to the same force as the specimen. The proportional limit of the strain bar is sufficiently high to insure that the strain in the bar follows Hooke's Law accurately under maximum loading conditions. Two strain gages of the same type as those employed on the specimen are bonded to the strain bar. The four gages on the specimen and strain bar are connected in a Wheatstone bridge circuit. This bridge is connected in such a way that the output signal is proportional to the difference between strains in the strain bar and in the specimen. The cross-section of the strain bar is such that the elastic strains in specimen and strain bar will almost cancel each other. The elastic strain signals will not exactly cancel because of small differences in areas and moduli of elasticity between the specimen and the strain bar, and small differences in the gage factors of the strain gages used.

Bending measurements were made before all tests in the rapid load testing machine by connecting the specimen gages to measure bending strains and loading the specimen to a stress well within the proportional limit of the specimen. After the bending strains were determined in this manner, the load on the specimen was decreased to the pre-load and the gages reconnected to measure tensile strains. All measured bending stresses were less than 5 per cent of the tensile stress in the specimen.

The output voltages from the strain bridge and the dynamometer bridge are amplified and then recorded on photographic paper by a recording oscillograph. This system is made up of standard equipment manufactured by the Consolidated Electrodynamics Corporation,

Pasadena, California, and includes the following:

1) Type 1-113B Bridge-Amplifiers, with incorporated antenuators to attenuate the signal after amplification, if necessary.

2) Type 2-105 Oscillator-Power Supply. The oscillator section supplies 3,000 cycles/sec at 10 volts for strain gage bridge excitation. The power supply section supplies power for the amplifiers and the oscillator.

3) Type 5-114-P2, 18 channel recording oscillograph. Paper speeds may be varied from 48 in./sec to 1/8 in./sec. Timing lines are projected at intervals of either 0.1 or 0.01 sec. The galvanometers, type No. 7-223, are fluid damped with a natural frequency of 835 cycles/sec.

The maximum sensitivity of the strain measurements in terms of strain in the specimen and trace deflection on the photographic paper with no attenuation is approximately 50×10^{-6} in./in. per inch of trace deflection. The maximum sensitivity of the load measurements in terms of load applied to the specimen and trace deflection is approximately 25 lb per inch of trace deflection. The trace deflections on the photographic record may be read to within $\pm$ 0.01 in. Therefore the test records can be read in terms of strain and load to within $\pm 0.5 \times 10^{-6}$ in./in. and $\pm$ 0.25 lb respectively. However, if the signal is attenuated in order that the trace deflection does not pass off the recording paper these sensitivities must be multiplied by the attenuation employed during the test.

A wire wound precision resistor of 100,000 ohms is used for calibration of both bridge circuits before and after a test. The cali-

bration resistor is shunted across one leg of the bridge by a suitable relay circuit which, in addition, starts the oscillograph. Therefore the trace deflection due to a known change in the resistance of one bridge leg is recorded. The calibration deflection of the trace may be converted to a known value of strain or load using the known resistance of the calibration resistor and the strain gages, and the calibration of the dynamometer or the gage factor of the strain gages.

IV. TEST PROCEDURE AND RESULTS

Tests were made at three temperatures; one group of specimens was tested at room temperature, one at -320°F, and several specimens were tested at -109°F. Specimens of all five grain sizes were tested at room temperature and -320°F, while specimens of only two grain sizes were tested at -109°F. Plastic deformation of the specimens tested at room temperature took place by slip. Plastic deformation by twinning was observed in specimens tested at -320°F. A small group of specimens was tested for -109°F for the purpose of determining the mode of plastic deformation occurring at this temperature. Plastic deformation occurred in these specimens in the same manner as the specimens tested at room temperature.

Two types of loading experiments were conducted at room temperature, one in which a constant load was rapidly applied, and one in which the specimen was loaded by small increments at five minute intervals. The first type will be referred to as rapid loading tests; the latter as static tests. Stress-strain curves were determined from the static tests. Strain was measured as a function of time in the rapid loading experiments, in order to measure the delay time for yielding.

Static Tests at Room Temperature

The stress was applied in increments of approximately 2500 lb/in^2. until a stress of the order of one half the proportional limit was attained. After reaching a stress equal to one half the

proportional limit, the stress increment was reduced to approximately 1000 lb/in^2. The strain and load were recorded approximately 5 minutes after a load increment was applied. The load was increased by the next increment immediately after recording these values.

The results of the static tests at room temperature for all grain sizes are presented in table II. Typical static stress-strain curves are plotted in figure 11.

A small amount of plastic strain, designated pre-yield microstrain, was observed at stresses just below the yield point in all static tests. The value of pre-yield microstrain at the upper yield point ranged from 30 to 150 x 10^{-6} in./in.

Rapid Loading Tests at Room Temperature

The rapid loading tests were performed with the rapid load testing machine. The specimen was subjected to a small preload in all rapid loading tests. The preload varied between 1000 lb/in.^{2} and 5000 lb/in.^{2} from test to test.

Delay time and the amount of microstrain at yielding were measured from the strain records of the tests performed on specimens of the three smallest grain sizes (d = 1.1, 2.4, and 4.3 x 10^3 in.).

A typical record of stress and strain as a function of time for a specimen which yielded is presented in figure 12. Plastic strain as a function of time for a specimen that did not yield is plotted in figure 13. Delay time and pre-yield microstrain are identified in figure 12. The results of the rapid loading tests performed on specimens of the

TABLE II

RESULTS OF STATIC TESTS PERFORMED AT ROOM TEMPERATURE

Specimen	Temperature ^{o}F	Average Grain Diameter 10^{-3} in.	Upper Yield Point 10^{3} lb/in.^{2}	Lower Yield Point 10^{3} lb/in.^{2}
25	73	1.1	30.4	26.5
30	76	1.1	32.2	23.2
31	75	1.1	34.5	24.6
33	75	1.1	34.5	22.0
M-2	78	2.4	21.8	19.1
L-2	72	2.4	22.6	18.8
M-4	74	2.4	24.0	19.2
M-6	72	2.4	26.3	23.2
5	76	4.3	14.7	13.6
6	76	4.3	15.1	14.2
4	75	4.3	15.4	14.5
K-6	72	5.5	14.4	13.4
E-6	70	5.5	15.1	14.2
A-7	78	5.5	15.1	14.4
A-3	72	5.5	15.6	14.7
E-7	76	5.5	16.3	14.7
J-4	71	8.1	-	9.8*
D-5	73	8.1	-	11.0*
B-6	72	8.1	-	11.1*
B-5	76	8.1	-	11.1*
J-8	72	8.1	-	11.3*
F-2	74	8.1	-	12.7*

* These values represent the stress at which the plastic strain equaled 200 x 10^{-6} in./in. An arbitrary value was chosen because of the absence of a yield point.

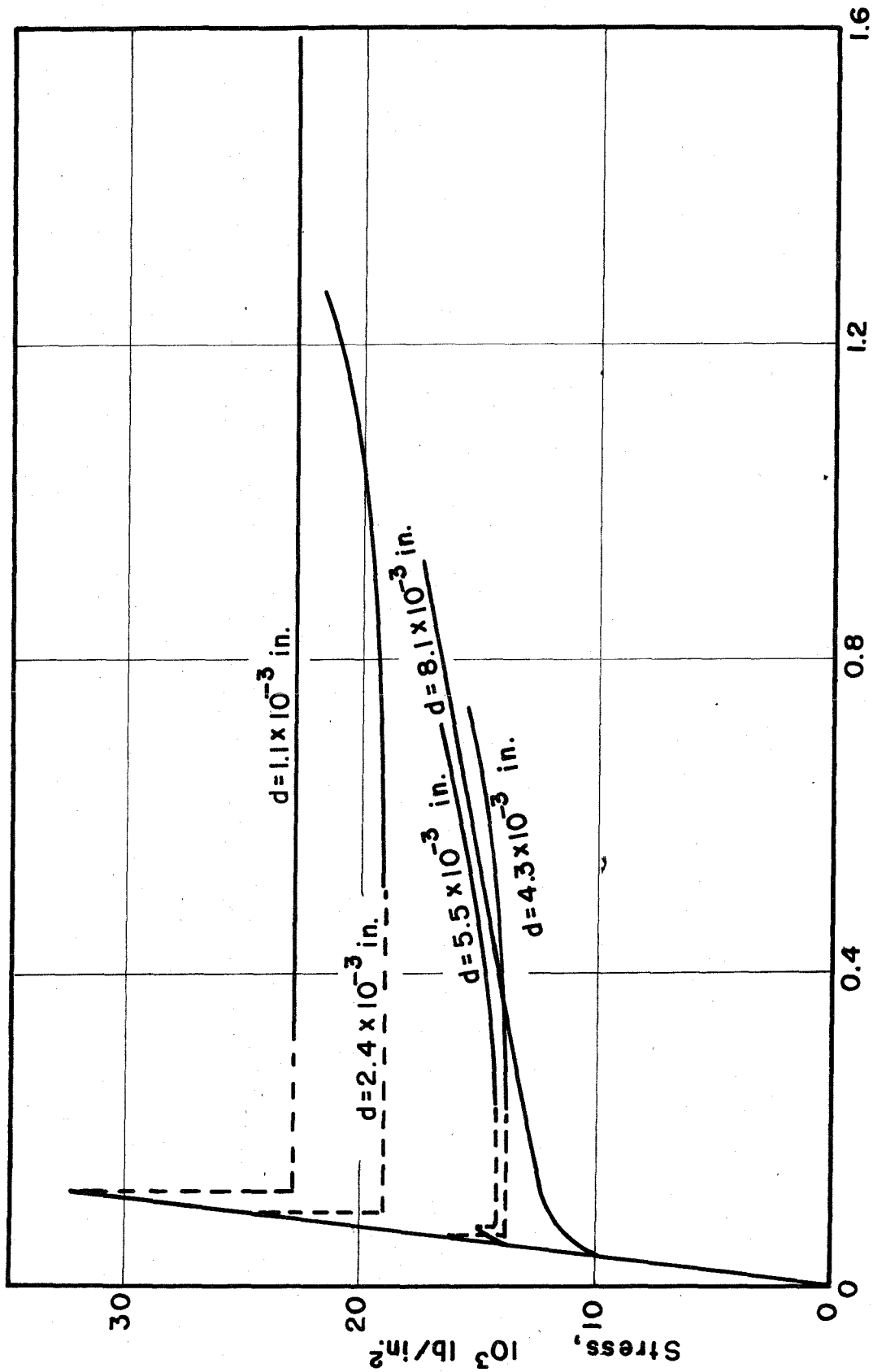

Fig. 11 Typical Static Stress - Strain Curves.

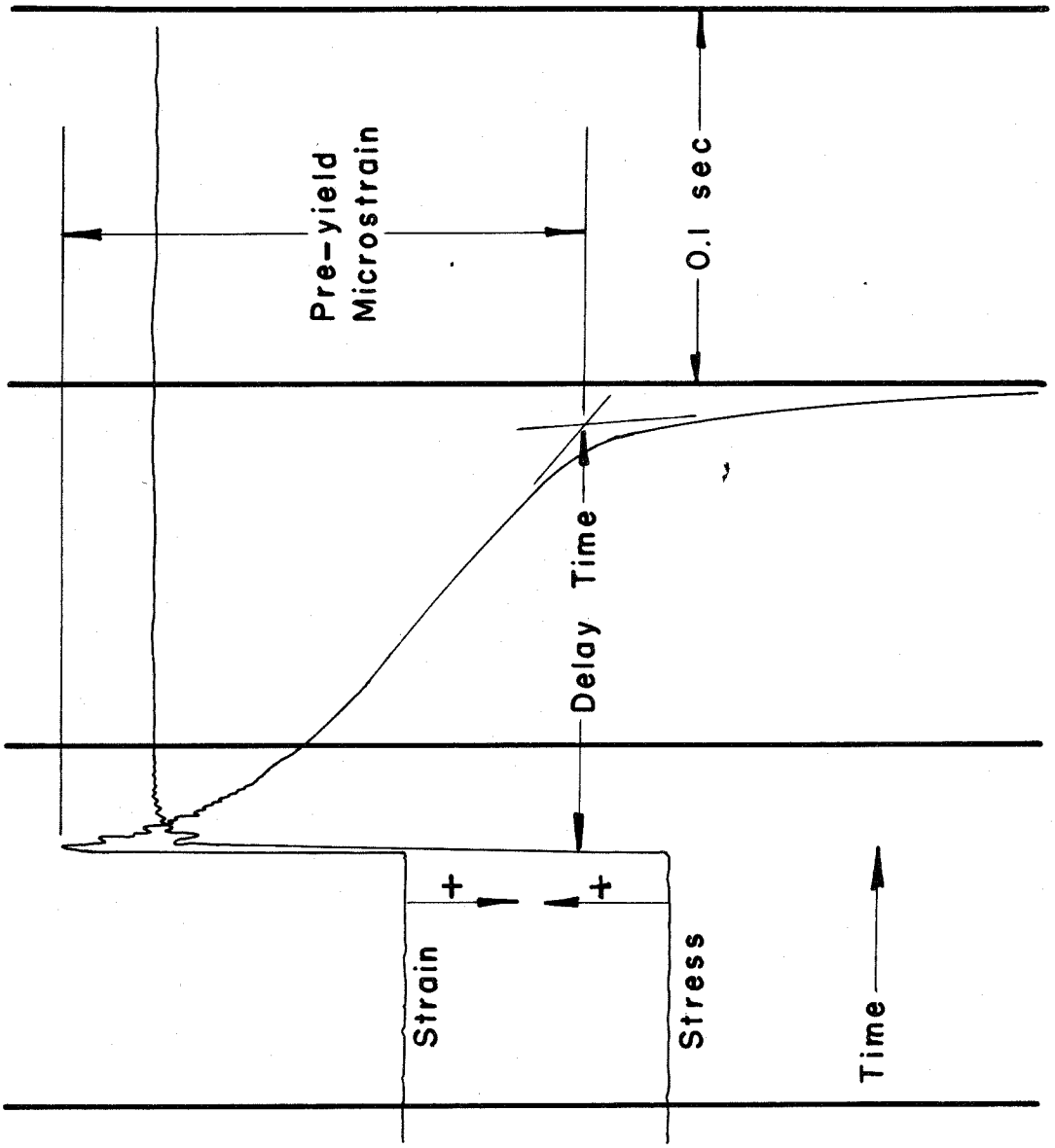

Fig. 12 Test Record for Material in which Yielding Occurred.

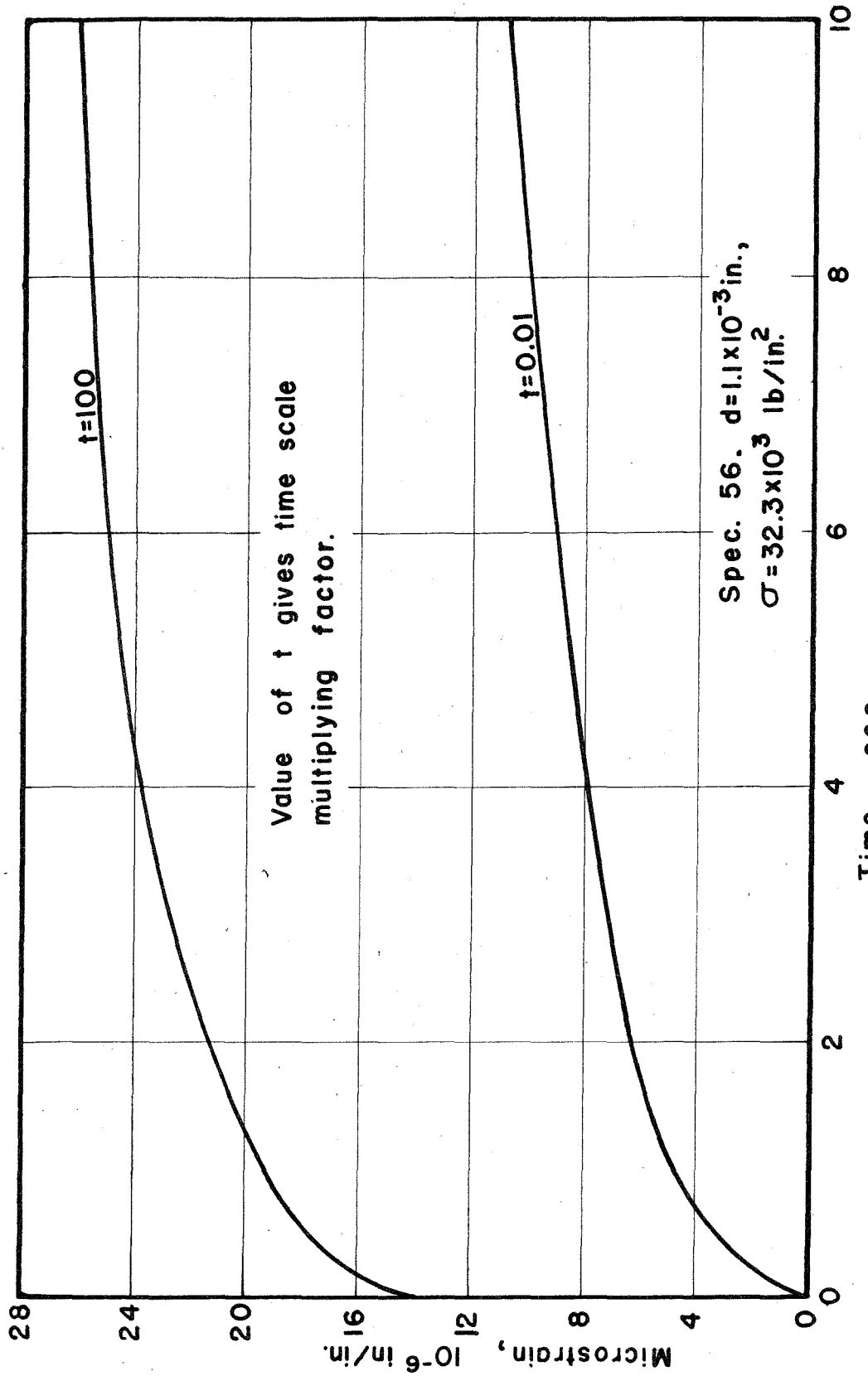

Fig. 13 Typical Curve of Microstrain vs. Time.
Stress just below Upper Yield Point.

three smallest grain sizes at room temperature are given in table III.

Specimens of the two largest grain sizes behaved somewhat differently in response to rapid loading. The specimens with average grain diameters of 8.1×10^{-3} and 5.5×10^{-3} in. plastically deformed by slip in such a way that plastic strain continued to increase with an increasing rate reaching large strain values (of the order of 500 to 1000×10^{-6} in./in.) before the strain rate began to decrease. The initial strain rate was zero or very small and the strain increased to values as large as $10,000 \times 10^{-6}$ in./in. with no sudden increase in rate. Consequently no delay time or pre-yield microstrain can be identified. Typical curves of plastic strain vs time for specimens which behave in this manner are presented in figure 14. Results of the rapid loading tests on specimens of the two largest grain sizes are given in table IV. The time reported in table IV is arbitrarily chosen to be the time after loading at which the plastic strain increased to 150×10^{-6} in./in.

An additional series of tests was performed for the purpose of establishing that specimen size was not responsible for the changes in deformation behavior observed with the larger grain sizes. Several specimens with a larger gage section were manufactured for these tests. Only one grain size was produced by recrystallization of these large specimens. The resulting average grain size in the large specimens was approximately equal to the largest grain size previously produced ($d = 8.1 \times 10^{-3}$ in.).

TABLE III

RESULTS OF RAPID LOADING TESTS AT ROOM TEMPERATURE

Specimen	Temperature ^{o}F	Average Grain Diameter 10^{-3} in.	Constant Applied Stress 10^{3} lb/in.^{2}	Delay Time Sec.	Microstrain at Yielding 10^{-6} in./in.
78	78	1.1	30.2	24	50
56	74	1.1	32.3	1000*	26*
44	72	1.1	33.8	1000*	23*
22	73	1.1	34.2	1.1×10^{-1}	130
77	75	1.1	35.2	12.3	80
79	77	1.1	36.2	8.2×10^{-2}	110
36	74	1.1	38.4	1.9×10^{-2}	60
75	78	1.1	39.1	2.8×10^{-2}	60
23	66	1.1	41.4	2.0×10^{-2}	-
24	72	1.1	42.5	9×10^{-3}	-
M-7	67	2.4	22.8	100*	25*
O-3	69	2.4	24.6	50	65
O-7	68	2.4	25.9	3.0×10^{-1}	90
O-2	70	2.4	29.1	1.4×10^{-1}	70
O-4	68	2.4	29.5	8.9×10^{-2}	80
O-5	71	2.4	31.8	3.8×10^{-2}	50
M-3	71	2.4	34.6	1×10^{-2}	50
O-6	70	2.4	39.1	5×10^{-3}	-
12	66	4.3	15.3	1000*	30*
60	78	4.3	16.6	133	80
59	80	4.3	16.7	150	80
55	82	4.3	16.8	4.1	150
21	65	4.3	17.1	2.7	65
81	80	4.3	17.1	10	150
20	70	4.3	18.9	1.8	100

TABLE III (Continued)

Specimen	Temperature ^{o}F	Average Grain Diameter 10^{-3} in.	Constant Applied Stress 10^{3} lb/in.^{2}	Delay Time Sec.	Microstrain at Yielding 10^{-6} in./in.
19	70	4.3	20.2	3.9×10^{-1}	60
82	75	4.3	24.8	8.0×10^{-2}	40
18	71	4.3	27.4	2.8×10^{-2}	100
83	76	4.3	30.6	9×10^{-3}	200
58	67	4.3	32.2	1×10^{-2}	-

* These times refer to the time the stress was held constant without yielding. The microstrain value is the strain measured at this time.

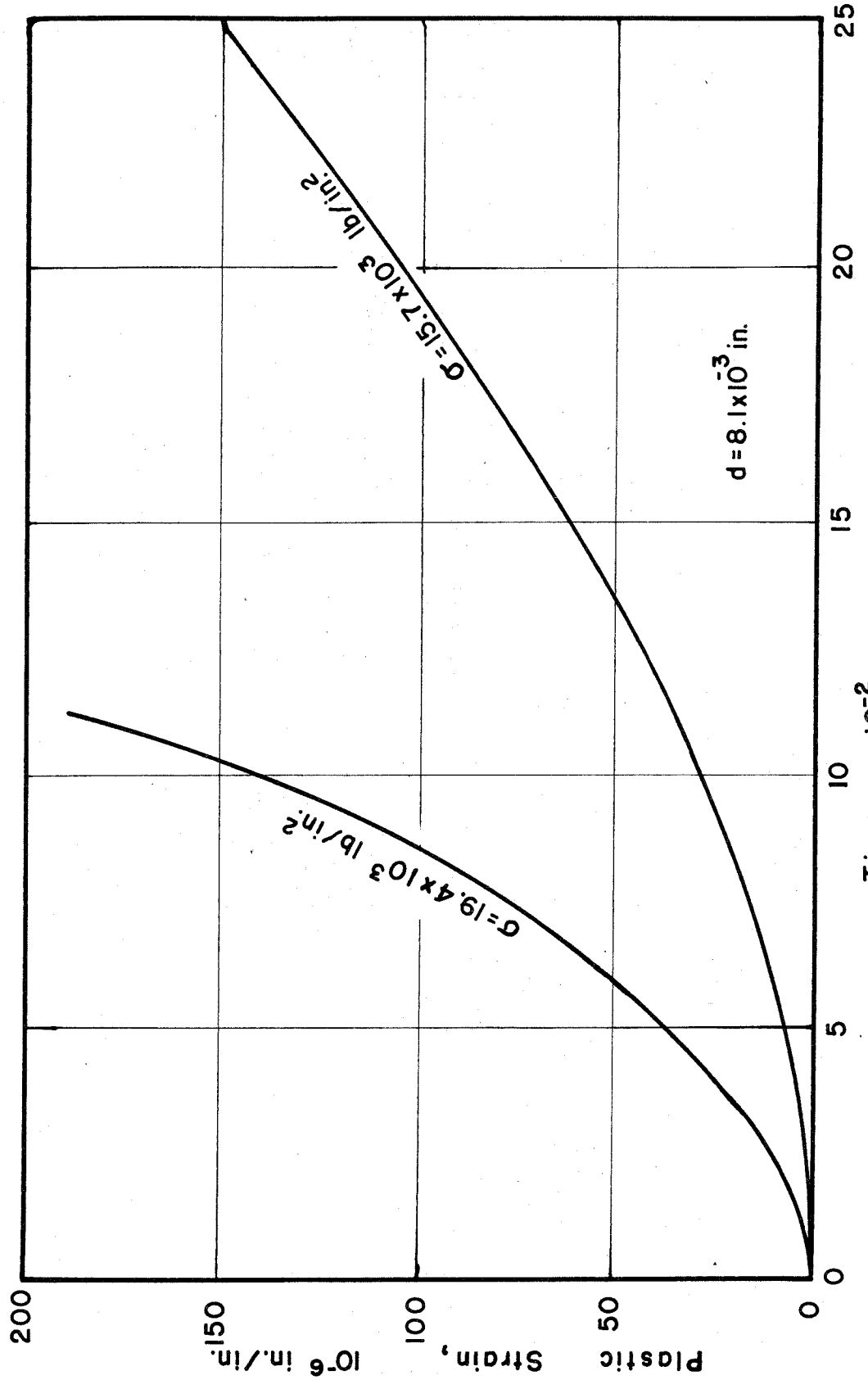

Fig. 14 Typical Curves of Strain vs. Time for Material without Yield Point.

TABLE IV

RESULTS OF RAPID LOADING TESTS AT ROOM TEMPERATURE

Specimen	Temperature ^{o}F	Average Grain Diameter 10^{-3} in.	Stress 10^{3} lb/in.^{2}	Time, t, for Strain to Reach Given Value Sec.	Strain at Time t 10^{-6} in./in.
C-6	68	8.1	9.5	60	28*
G-4	70	8.1	10.1	180	120*
B-7	68	8.1	10.6	800	120*
B-4	70	8.1	11.3	500	60*
C-4	66	8.1	11.3	6.5	150
G-3	70	8.1	11.8	26	150
D-2	67	8.1	15.7	2.5×10^{-1}	150
I-4	76	8.1	17.2	2.9×10^{-1}	150
C-2	76	8.1	17.2	2.6×10^{-1}	150
C-3	69	8.1	19.4	1.1×10^{-1}	150
G-2	68	8.1	19.5	8.0×10^{-2}	150
E-3	68	5.5	13.9	284	44*
E-5	64	5.5	19.1	1.1	150
E-2	69	5.5	20.2	1.2×10^{-1}	150
Special Specimens with Larger Gage Sections					
V-4	72	8.1	10.1	1200	35*
IX-4	68	8.1	11.6	220	150
X-5	70	8.1	13.1	17	150
II-2	72	8.1	13.5	7.5	150
VI-4	73	8.1	14.7	2.3	150
III-2	70	8.1	14.9	2.0	150
I-3	70	8.1	19.1	1.8×10^{-1}	150

* These strain values represent the maximum strain recorded in the test.

Testing of the large specimens was performed in another rapid load testing machine which is capable of producing the greater loads which were necessary due to the larger cross-sectional area of the specimens. This machine was constructed for use in earlier work in the Dynamic Properties Laboratory of the California Institute of Technology (19).

The results of the tests, using the larger specimens, are also given in table IV. A comparison of these results with the results of tests performed on smaller specimens indicates that the behavior of the specimens of larger grain sizes is truly related to the effect of grain size and is not affected by the specimen size.

Tests at -320°F

All tests at -320°F were performed in the rapid load testing machine. The temperature was held at -320°F by submerging the lower end of the testing machine, including the specimen and strain bar, in a vessel of boiling liquid nitrogen. The gages used for strain measurement at this temperature were Baldwin SR-4, FA-4, and FA-2 foil resistance strain gages. The regular wire gages (A-7 and A-18) used at room temperature were not serviceable at -320°F because of gage failure at very small stresses. Foil gages proved satisfactory up to an elastic stress in steel of the order of 80,000 $lb/in.^2$. The foil gages were bonded to the specimens with an epoxy resin.

Strain gages at -320°F are extremely sensitive to temperature changes. The signal resulting from a temperature change of

approximately 0.003°F at one gage is equivalent to the signal resulting from a strain of 1 x 10^{-6} in./in. As a result of this temperature sensitivity the formation and departure of gas bubbles at the gage surface and small convection currents in the liquid nitrogen bath resulted in a noise output of the order of 50 x 10^{-6} in./in. This difficuly was eliminated by isolating the strain gage surfaces from direct contact with the liquid nitrogen bath. Isolation was accomplished by first covering the gages with a frame of cardboard and then wrapping the gage section with two or three layers of saran wrap. The saran was held in place by thread and the edges sealed with a small quantity of silicone vacuum grease. This procedure eliminated the rapid fluctuations of the strain gage bridge signal. Slower drifting fluctuations were reduced to the order of 5 to 10 x 10^{-6} in./in.

Three types of tests were employed in testing specimens -320°F: 1) Rapid loading tests; 2) Static tests; 3) Interrupted loading tests. The rapid loading tests were conducted in the same way as tests performed at room temperature. The static tests at this temperature were not conducted in the same manner as the tests at room temperature. The static tests at -320°F were performed in the rapid load testing machine. The load was slowly increased at a constant rate by bleeding high pressure gas into the lower pressure chamber of the machine. Stress rates in the static tests varied from test to test but were in the range from 500 to 1500 lb/in.^{2} sec. The interrupted loading tests were also performed in the rapid load testing machine. These tests involved loading specimens to a given stress, as in the

static tests, then holding at this stress for 1/2 hr before slowly increasing the stress again at a constant rate.

Initiation of plastic deformation at -320° F in specimens of the four largest grain sizes occurred in the same general manner. Strain records from rapid loading tests show that there was no plastic deformation (within the accuracy of measurement) if the stress was less than a critical value. If the stress in the specimen exceeded this critical value, a large amount of plastic deformation (500 to 2000 x 10^{-6} in./in.) occurred in a period of approximately 0.001 sec after the load was applied.

Large plastic strains also occurred very rapidly when the stress reached a critical value in the static and interrupted tests. Plastic strain was not observed at stresses less than the critical value. An audible cracking sound was observed with the rapid deformation in the static and interrupted tests. The critical stresses for the initiation of plastic deformation measured in all three types of tests were approximately equal for a particular grain size. Metallographic examination of specimens of the four largest grain sizes which had been plastically deformed, revealed numerous twins in the structure, uniformly distributed over the gage length. Figure 15 shows a typical microstructure after plastic deformation at -320° F.

Specimens of the smallest grain size (average diameter = 1.1 x 10^{-3} in.) behaved somewhat differently than specimens of the larger grain sizes. Rapid loading tests on these specimens produced twinning only in regions of severe slip or fracture. Strain measurements were not made in these tests. However, metallographic examination revealed

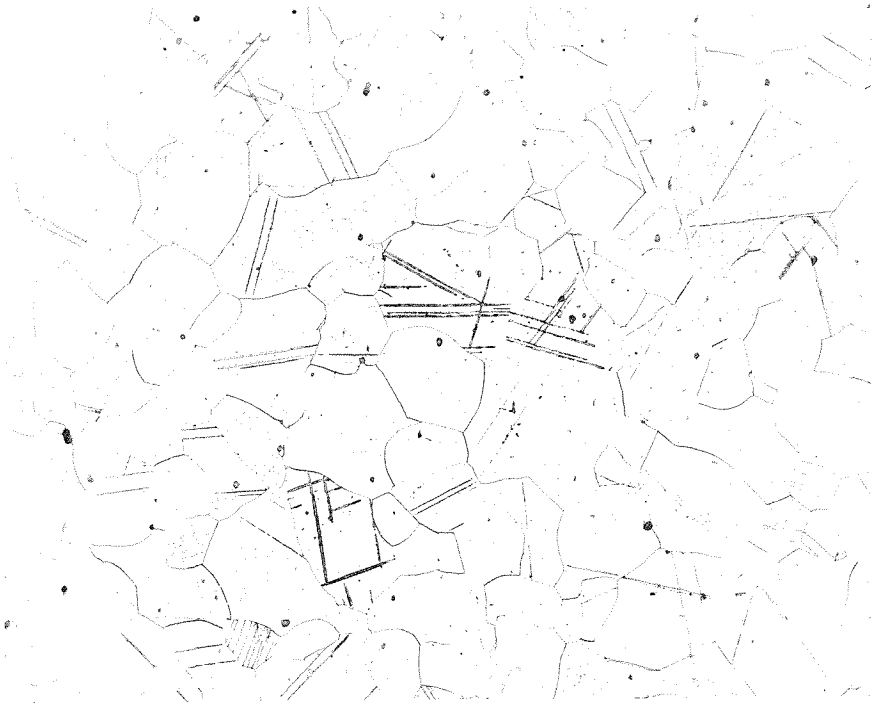

Fig. 15 Microstructure after Plastic Deformation at -320°F. 150X.

twinned areas only in necked down regions, at the ends of the gage section or in close proximity to a fracture surface.

The results of the tests performed at -320° F are given in table V and VI.

Rapid Loading Tests at -109° F

Six rapid loading tests were performed at a temperature of -109° F on specimens having average grain diameters of 2.4×10^{-3} and 8.1×10^{-3} in. The temperature was held constant by submerging the lower end of the testing machine in a bath of liquid Freon 12 and solid carbon dioxide. The results of these six tests are given in table VII. Only plastic deformation by slip was observed. Strain vs. time records indicated a behavior similar to the tests at room temperature. Tests on specimens of the smaller grain sizes exhibited a definite delay time preceded by a decreasing microstrain rate. The specimens of the larger grain sizes exhibited no delay time. No twinning was observed during or after these tests.

TABLE V

RESULTS OF RAPID LOADING TESTS PERFORMED AT -320°F

Specimen	Average Grain Diameter 10^{-3} in.	Constant Applied Stress 10^{3} lb/in^{2}	Result*
I-5**	8.1	30.2	No Twinning
I-5	8.1	44.0	No Twinning
H-2**	8.1	31.6	No Twinning
H-2	8.1	53.2	No Twinning
H-2	8.1	71.2	Twinning
F-6**	8.1	58.2	No Twinning
F-6	8.1	62.3	Twinning
J-5	8.1	56.5	No Twinning
F-4	8.1	59.4	Twinning
F-5	8.1	59.7	Twinning
F-3	8.1	63.6	Twinning
J-6	8.1	65.1	Twinning
J-7	8.1	65.6	Twinning
K-3	5.5	59.4	No Twinning
K-4	5.5	60.9	No Twinning
K-1	5.5	63.6	Twinning
K-2	5.5	77.3	Twinning
N-7	2.5	56.4	No Twinning
N-3	2.5	68.0	No Twinning
N-4	2.5	79.2	No Twinning
N-5	2.5	79.0	Twinning
N-2	2.5	86	Twinning
73	1.1	87.3	No Twinning
74	1.1	102.5	Twinning in necked down region

TABLE V (Cont'd)

71	1.1	104.0	Twinning at ends of gage section
72	1.1	110.0	Twinning at ends of gage section
61***	1.1	99.7	No Twinning
64***	1.1	104.5	No Twinning
63***	1.1	118.5	Twinning in necked down region
62***	1.1	118.5	Twinning at fracture

* Twinning was observed to occur uniformly throughout the gage section, unless otherwise noted.

** Specimens were loaded two or more times in sequence and were held at -320°F between tests.

*** These specimens were not decarburized, carbon content equaled approximately 0.09%.

TABLE VI

RESULTS OF STATIC AND INTERRUPTED TESTS PERFORMED AT -320°F

Specimen	Type of Test	Average Grain Diameter 10^{-3} in^2	Constant Stress in Interrupted Tests 10^3 lb/in^2	Time that Stress was Held Constant in Interrupted Tests Sec	Stress at which Twinning Occurred 10^3 lb/in^2
H-4	Interrupted	8.1	52.9	1820	62.6
G-6	Interrupted	8.1	54.3	1950	63.2
H-3	Interrupted	8.1	56.9	2070	63.6
H-6	Static	8.1	-	-	65.3
A-5	Static	5.5	-	-	71.4
A-8	Static	5.5	-	-	69.3
14	Static	4.3	-	-	61.3
11	Static	4.3	-	-	62.6
13	Static	4.3	-	-	63.6
N-6	Static	2.5	-	-	80.4

TABLE VII

RESULTS OF RAPID LOADING TESTS AT -109°F

Specimen	Average Grain Diameter 10^{-3} in.	Constant Applied Stress 10^{3} lb/in^{2}	Delay Time Sec	Microstrain at Yielding x 10^{-6} in/in
L-7	2.5	47.8	1	100
L-1	2.5	49.8	3.8×10^{-1}	160

Specimen Specimen	Average Grain Diameter 10^{-3} in.	Constant Applied Stress 10^{3} lb/in^{2}	Time, t, for Strain to Reach given Value Sec	Strain at Time t x 10^{-6} in/in
K-8	5.5	25.0	120	150
K-9	5.5	25.0	150	150
A-1	5.5	25.7	21	150
A-4	5.5	31.1	4.0	150

V. DISCUSSION OF RESULTS

A variation of the static upper and lower yield points with grain size was observed in this investigation and is reported in table II. This data is presented in figure 16 with the upper and lower yield points plotted as a function of $d^{-1/2}$, where d is the average grain diameter. Both the upper and lower yield points can be interpreted to be a linear function of $d^{-1/2}$.

Figure 16 shows that the two lines representing the values of the lower and upper yield points intersect at $d \cong 8 \times 10^{-3}$ in. The intersection of these two lines indicates that the initiation of plastic deformation in specimens of a grain size larger than $d \cong 8 \times 10^{-3}$ in. will be different from that observed in specimens of a smaller grain size. This conclusion is borne out by the fact that the specimens of $d = 8.1 \times 10^{-3}$ exhibit no yield point. Holden and Hollomon (3) have shown that the yield point is also absent in tensile tests on single crystals. Therefore it may be concluded that for a given steel there is no yield point in specimens of an average grain diameter larger than some particular value. This value is $d \cong 8 \times 10^{-3}$ in. for the steel used in this investigation.

The behavior of the lower yield point as a function of grain size is in qualitative agreement with the results reported by Petch (14), Hall (15) and Low (16). These investigators do not report any relationship for the upper yield point, assuming that the lower yield point is the only value of significance.

The influence of grain size on the static yield point observed in this investigation is compatible with a dislocation mechanism originally proposed by Cottrell (13). The general aspects of Cottrell's mechanism

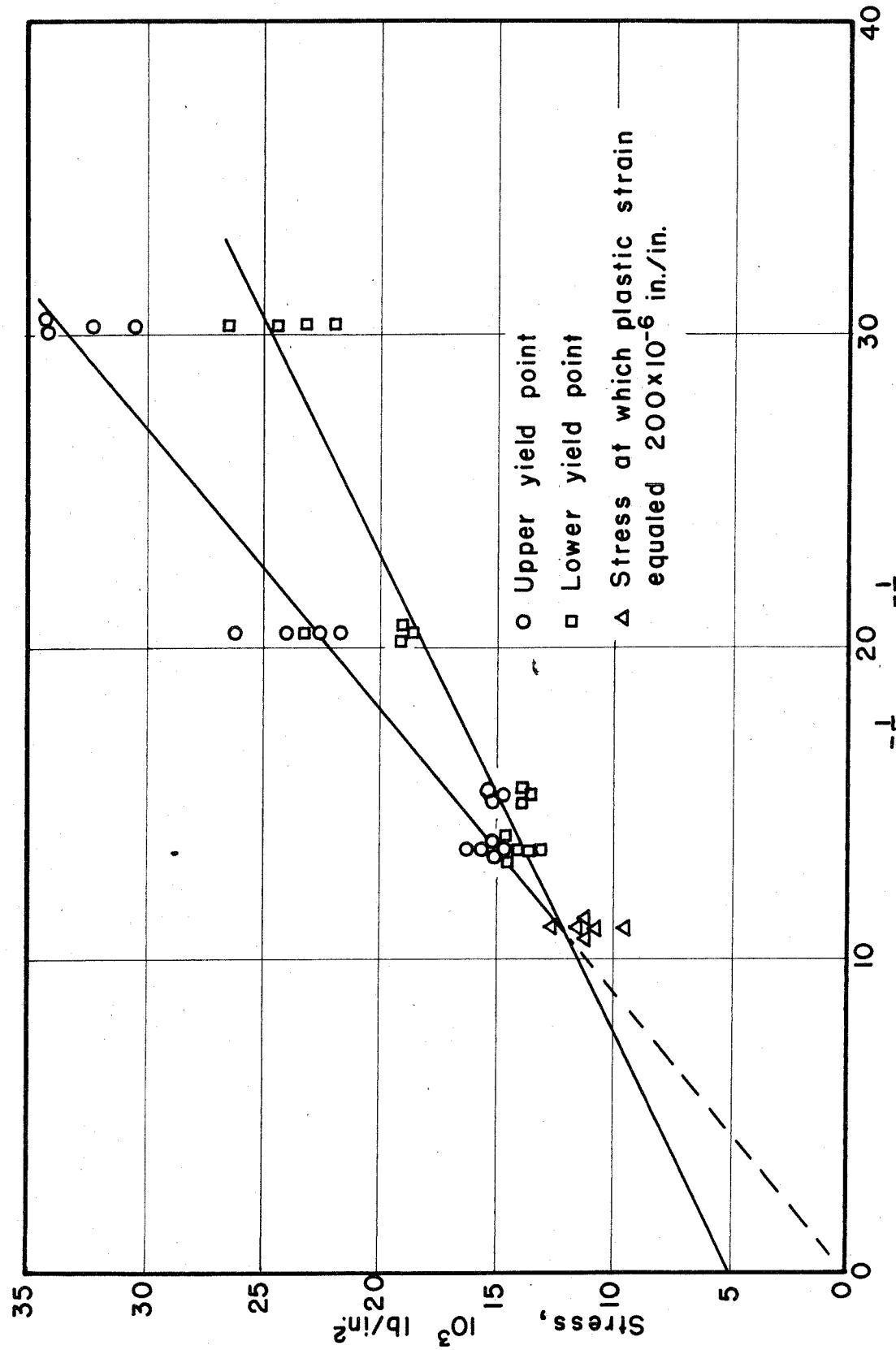

Fig. 16 Upper and Lower Yield Point vs. Inverse Square Root of Average Grain Diameter.

can be summarized in the following way:

A Frank-Read dislocation source in a body centered cubic lattice will be surrounded by an atmosphere of interstitial impurity atoms, such as carbon or nitrogen in α-iron. Under the influence of a suitably applied stress, a segment of a source can expand in its slip plane once the interaction stresses between the segment and the atmosphere has been overcome. Once the loop is able to move freely it will form a complete ring around the source and move radially outward under the action of the applied stress. The applied stress required for the generation of dislocation rings is smaller than predicted from considerations of the interaction forces between a dislocation and its atmosphere. The lower applied stress is the result of the effect of thermal vibrations within the crystal lattice. A suitable thermal vibration will provide additional energy for the generation process. Hence, the value of the applied stress required for generating a dislocation ring will be much smaller than the value required in the absence of thermal vibrations. The generated dislocation ring will expand radially in its slip plane under the action of an applied stress until an obstacle is encountered. When an obstacle blocks the motion of a dislocation ring, additional stress must be applied if the ring is to expand further. Grain boundaries, foreign particles, other dislocations, would all offer resistance to dislocation motion.

Cottrell suggests that generated dislocation rings will move outward in their slip plane until stopped by collision with a grain boundary. As additional rings are generated and move outward from the source, a pile-up of dislocations will occur at the grain boundary. This pile-up

increases until one of two things occurs: 1) The stress at the source decreases to a value where further generation is impossible; 2) The local stress at the grain boundary due to the pile-up of dislocations becomes so great that the grain boundary barrier can be overcome. As the pile-up of dislocations at the grain boundary increases the stress at the source will decrease due to the "back" stress of the previously generated dislocations. If the stress at the source decreases to the point that further dislocation generation is impossible, the process will stop and yielding will not occur. When the number of dislocations at the grain boundary is sufficient to increase the local stress at the boundary to the point that slip is initiated in the next grain, yielding will occur. Therefore yielding will take place if the applied stress is large enough to allow generation of a critical number of dislocations before the source becomes inactive.

The observed influence of grain size on the static yield point can be easily explained in terms of the mechanism suggested by Cottrell. Petch (14) has suggested a treatment of Cottrell's mechanism that gives an expression for the lower yield point as a function of grain size, but in his treatment the upper yield point is neglected. A more detailed treatment of Cottrell's mechanism than suggested by Petch will not only account for the lower yield point but will suggest a model for both the upper and lower yield points.

According to Cottrell's yielding mechanism, at the static yield point the dislocations piled up at an obstacle will be in equilibrium. The source which generated these dislocations will be inactive. The length of a pile-up of dislocations under an applied stress has been calculated by Eshelby,

Frank, and Nabarro (20) and is given by

$$L = \frac{Gbn}{\pi \tau} \tag{1}$$

where G = the shear modulus

b = the atomic slip distance or Burgers vector

n = the number of dislocations in the pile-up

τ = the resolved shear stress acting on the dislocations in the pile-up.

If one assumes that there is a drag or friction force on each dislocation, then equation 1 may be rewritten

$$L = \frac{Gbn}{\pi(\tau - \tau_i)} \tag{2}$$

where τ_i = the stress due to friction or drag forces on each dislocation.

The drag stress is the result of minor obstacles which retard dislocation motion in the slip plane.

A pile-up of dislocations produces a stress concentration in the vicinity of the obstacle causing the pile-up. An expression for the maximum stress at the front of a pile-up has also been given by Eshelby, Frank, and Nabarro (20). Taking this expression and again assuming that there is a drag force on the dislocations results in

$$\tau_b = n(\tau - \tau_i) \tag{3}$$

where τ_b = the local stress at the front of a pile-up of dislocations.

When the assumption is made that a critical resolved shear stress, τ_b^*, must be achieved to initiate yielding, then the required number of

dislocations in the array is given by

$$n^* = \frac{\tau_b^*}{(\tau_y - \tau_i)} \tag{4}$$

where τ_y = the resolved applied shear stress at yielding.

Combining equations 2 and 4 gives

$$L^* = \frac{Gb\tau_b^*}{\pi(\tau_y - \tau_i)^2} \tag{5}$$

L^* in equation 5 represents the minimum length of slip plane that is necessary for a pile-up of n^* dislocations to occur under the action of an applied stress equal to τ_y. Rewriting equation 5 gives

$$\tau_y = \tau_i + \sqrt{\frac{Gb\tau_b^*}{\pi L^*}} \tag{6}$$

L^* is related to the distance from a source to an obstacle producing a dislocation pile-up. If this distance is proportional to the grain size, then $L^* = fd$, where f is a proportionality constant and d is the average grain diameter. Substituting this expression for L^* into equation 6 gives

$$\tau_y = \tau_i + kd^{-\frac{1}{2}} \tag{7}$$

where $$k = \sqrt{\frac{Gb\tau_b^*}{\pi f}}$$

In the expression for τ_y given in equation 7 τ_y is a linear function of $d^{-1/2}$. This is in agreement with the experimental results of this investigation, which are plotted in figure 16. The expression

for the stress at yielding (τ_y) given by equation 7 describes the variation of both the upper and lower yield points with grain size. Therefore it may be postulated that both the upper and lower yield points are governed by the piling up of dislocations at obstacles. If the expression in equation 7 is to represent both the upper and lower yield point, a more detailed model than Cottrell's model must be postulated for the initiation of yielding.

The upper yield point is the result of dislocations piling up at a grain boundary. When the local stress at the boundary increases to a critical value, slip in the next grain will be initiated and catastrophic slip across successive grains will result. The applied stress that will cause dislocations to break through a grain boundary and initiate slip in successive grains is the upper yield point.

As slip in several grains becomes more general, after grain boundary break through, many dislocations move on several sets of slip planes. Two dislocations will interact as they move in intersecting planes and approach the intersection of the slip planes. If the dislocations are of the type shown in figure 17a their motion is stopped by the interaction force and the dislocations come to rest in an equilibrium position. Additional stresses in these slip planes are necessary to overcome the interaction of the two dislocations and allow them to move together, and finally pass. Two dislocation pile-ups, such as shown in figure 17b, will result as additional dislocations arrive at the intersection of the slip planes. The dislocations at the front of each pile-up will move closer together, finally forming one sessile dislocation, as the number of dislocations in each pile-up increases.

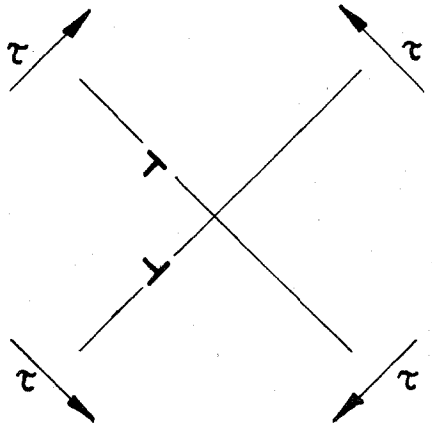

(a) Initial Condition.

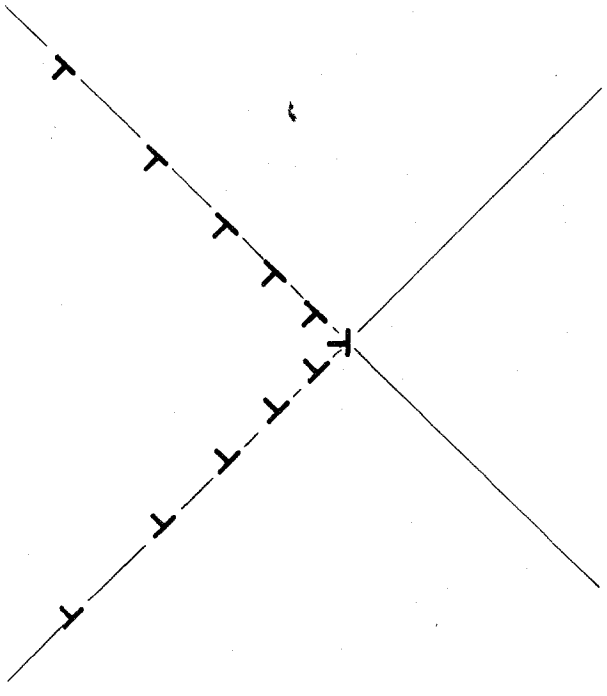

(b) Final Condition.

Fig. 17. Schematic Representation of the Formation of Dislocation Pile-Ups at an Intersection of Two Slip Planes.

The dislocations will continue moving in their slip plane only when the local stress is large enough to allow the sessile dislocation to dissociate into two mobile dislocations. This collision mechanism therefore constitutes a second set of obstacles which retards dislocation motion. The obstacle resulting from the formation of a sessile dislocation can only be overcome if a dislocation pile-up is formed which will produce a stress concentration of sufficient magnitude. The applied stress required to produce pile-ups of a sufficient magnitude to allow slip on intersecting planes can be interpreted as the lower yield point. Therefore the lower yield point is the minimum stress necessary to continue plastic deformation after it has been initiated at the upper yield point.

The disappearance of the yield point in specimens of larger grain sizes can also be explained in terms of this model. As the grain size is increased, the probability of dislocations colliding within a single grain before encountering a grain boundary is also increased. Thus in large grains many dislocation pile-ups will occur initially at slip plane intersections instead of grain boundaries. The slip mechanism will therefore be reversed from that visualized for small grained specimens in that the primary obstacles to slip will be sessile dislocations and not grain boundaries. When the stress is sufficient to allow the sessile dislocation to dissociate into mobile dislocations, the number of dislocations free to move will be so large that the grain boundary cannot offer appreciable resistance to their motion. Consequently this model can account for the disappearance of the yield point in specimens of large grain size.

When no yield point exists, the stress values which will cause slip are given by equation 5.

The extrapolation of the line representing the upper yield point vs. $d^{-1/2}$ in figure 16 passes through the origin, hence τ_i, the friction stress or drag stress, is approximately zero. This can be interpreted to mean that if the upper yield point is the result of grain boundary pile-ups, then the drag on free dislocations moving from a source to the grain boundary is very small.

Fitting the slope of equation 7 to the experimental data for the upper yield point, gives a value of $k = 5.55 \times 10^2 lb/in^{3/2}$. The factor fd, representing the average distance from randomly distributed dislocation sources to grain boundaries in a given set of parallel slip planes, may be calculated. The result of this calculation, presented in Appendix B, gives $f = 0.12$. Substituting $G = 12 \times 10^6 lb/in^2$., $b = 0.985 \times 10^{-8}$ in., $f = 0.12$ and the experimentally determined value for k into the expression for k gives $\tau_b^* = 0.99 \times 10^6 lb/in^2$. This value of τ_b^* represents the stress required to activate the slip process in the next grain and thereby initiate yielding. This value is of the same order as the stress which has been calculated (21) and observed (22) to produce plastic deformation in a perfect single crystal. Therefore the value of τ_b^* resulting from fitting the theoretical expression for the static upper yield point to the experimental data is of a reasonable magnitude.

The experimental data for the static lower yield point gives $\tau_i = 2,500\ lb/in^2$. This value is in good agreement with the stress reported by Holden and Hollomon (3) to slip a large single

crystal of iron, with or without carbon as an impurity.

The values of stress which caused plastic slip in the specimens not exhibiting a yield point, ($d = 8.1 \times 10^{-3}$ in.) are observed to fall close to the extension of the lower yield point curve in figure 16. Equation 7 therefore represents not only the lower yield point but also the stress which causes slip in grain sizes not exhibiting a yield point. This is in accord with the yielding model previously discussed.

Fitting the slope of equation 7 to the data for the lower yield point gives $k = 3.38 \times 10^{2}$ lb/in.$^{3/2}$. Taking this experimentally determined value of k and using the same values as before for G and b gives $\tau_b^* = 3.0 \times 10^{6}$ (f) lb/in^2 for the lower yield point. According to the proposed model this value of τ_b^* represents the stress required to overcome the resistance to dislocation motion resulting from dislocation collisions on intersecting slip planes. The physical interpretation of f is more difficult in this case than it was for the upper yield point. The factor f has not been calculated. However, taking it to be approximately 0.1 gives $\tau_b^* = 0.3 \times 10^{6}$ lb/in^2., for the lower yield point.

The interaction force between two dislocation arrays on intersecting slip planes can be roughly estimated in order to check the value of τ_b^* for the lower yield point obtained from the experimental data. This estimate is made by considering the simpler problem of the interaction of two dislocations on intersecting planes.

In the type of material under study, namely the body centered cubic crystal structure, there are many slip systems which offer the possibility of intersecting slip planes. There is an elastic interaction force between many of the dislocations which can move in

these intersecting slip planes. The stress required to force two dislocations on different intersecting planes together to the point that their cores are just touching can be easily calculated if the interaction of the cores is neglected.

The interaction stress between dislocations in the $\{110\}$ planes which meet at the intersection of these planes has been calculated. The intersections of $\{110\}$ planes will fall on lines in the $\langle 100 \rangle$ direction or the $\langle 111 \rangle$ direction. Therefore dislocations lines parallel to these directions are considered. The Burgers vectors of the dislocations to be considered are of the type $\frac{a}{2}\langle 111 \rangle$ in all cases. The calculation of the interaction stress between two dislocations which come together along a line in the $\langle 100 \rangle$ direction will be outlined in the following paragraph. The interaction forces between dislocations meeting in the $\langle 100 \rangle$ directions can be calculated in a similar manner.

Consider two dislocations which lie in intersecting $\{110\}$ planes and are parallel to the $\langle 100 \rangle$ direction. These dislocations will have both screw and edge components in the $\langle 100 \rangle$ direction. The screw components of the two dislocations may be of the same sign or of opposite sign. However, whether the screw components attract or repel the maximum force required to force the dislocations together or to separate them is the same. The edge and both possible screw components are shown in figure 18a. The sum of the interaction forces between components will be equal to the total interaction force between dislocations. Assuming the coordinate system shown in figure 18b, the force in the y direction on dislocation 2 due to the stress field of the edge component of dislocation 1 is

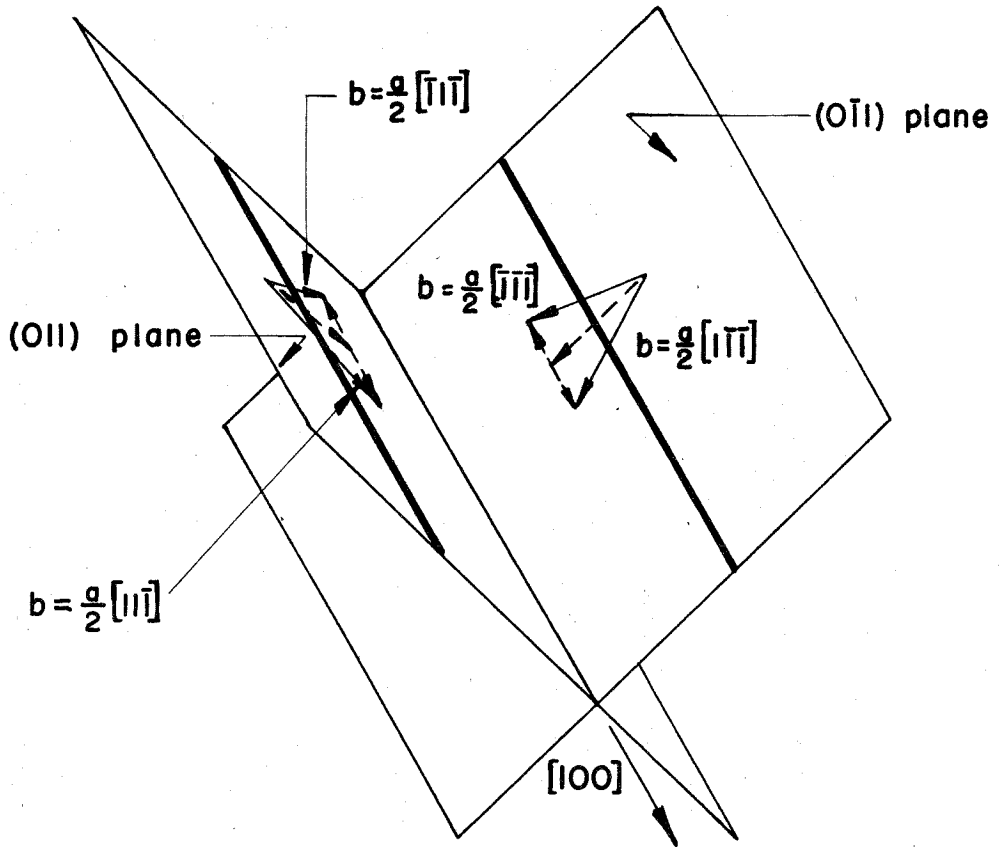

(a) Crystallographic Coordinate System.

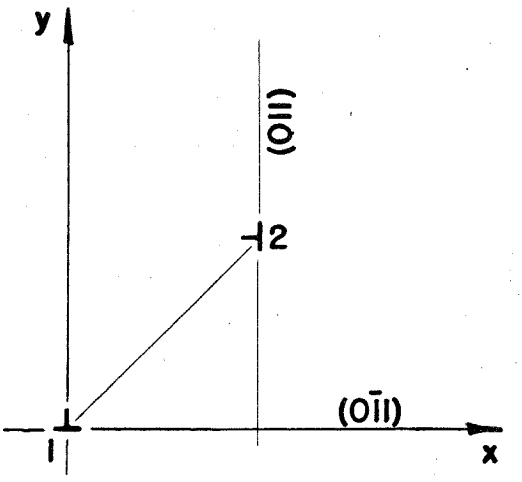

(b) Cartesian Coordinate System.

Fig. 18 Schematic Representation of Two Dislocations at Equilibrium near the Intersection of Two Slip Planes.

$$F_y = \frac{G b_e^2}{2\pi(1-\upsilon)} \frac{x(x^2-y^2)}{(x^2+y^2)^2} \tag{8}$$

where $b_e = \frac{\sqrt{2}}{\sqrt{3}} b$ = the edge component of the Burgers vector of the slip dislocation

υ = Poisson's ratio.

If $x = y$ then $F_y = 0$. Therefore, the edge component of dislocation 1 will not interact with dislocation 2.

The force on dislocation 2 resulting from the screw component of dislocation 1 is given by

$$F_y = \frac{G b_s^2}{2\pi} \frac{x}{(x^2+y^2)} \tag{9}$$

where $b_s = \frac{b}{\sqrt{3}}$ = the screw component of the Burgers vector of the slip dislocation.

This is the only interaction force between these dislocations when $x = y$. Therefore, the stress necessary to force the dislocations to a position where their centers are 4b apart is

$$\tau = \frac{G}{8\pi\sqrt{6}} \cong 0.2 \times 10^6 \text{ lb/in}^2 \tag{10}$$

Similar calculations for three other cases involving dislocations which are parallel to the <111> direction give interaction stresses of approximately 0.2×10^6 lb/in^2. for two cases and 0.5×10^6 lb/in^2. for the other.

These calculated values and the experimentally determined value of τ_b^*, for the lower yield point, are approximately equal. Therefore it appears that the more detailed model of Cottrell's yielding mechanism presented here can explain the values of the lower yield point observed in this investigation.

The experimental observations of this investigation of the static upper and lower yield points may be explained by the proposed extension of Cottrell's model. The upper yield point is the stress required to produce a dislocation pile-up at a grain boundary of sufficient magnitude to initiate slip in successive grains. The lower yield point is the stress required to produce dislocation pile-ups of sufficient magnitude to drive colliding dislocations past each other. Therefore, large plastic deformations are initiated at the upper yield point and the lower yield point is the stress necessary to continue this initial plastic deformation.

The results of the rapid loading tests obtained in this investigation provide more information for the study of the yielding mechanism. The existence of a delay time for yielding after rapid loading a specimen to above the static upper yield point supports Cottrell's general yielding mechanism. According to Cottrell's mechanism the delay time is the time required to pile up a sufficient number of dislocations at a grain boundary to initiate slip in successive grains. The generation of a given number of dislocations requires that sufficient time elapse in order that the necessary number of thermal vibrations can occur at the dislocation source.

The delay times observed in this investigation are plotted as a function of applied tensile stress in figure 19. Only the results

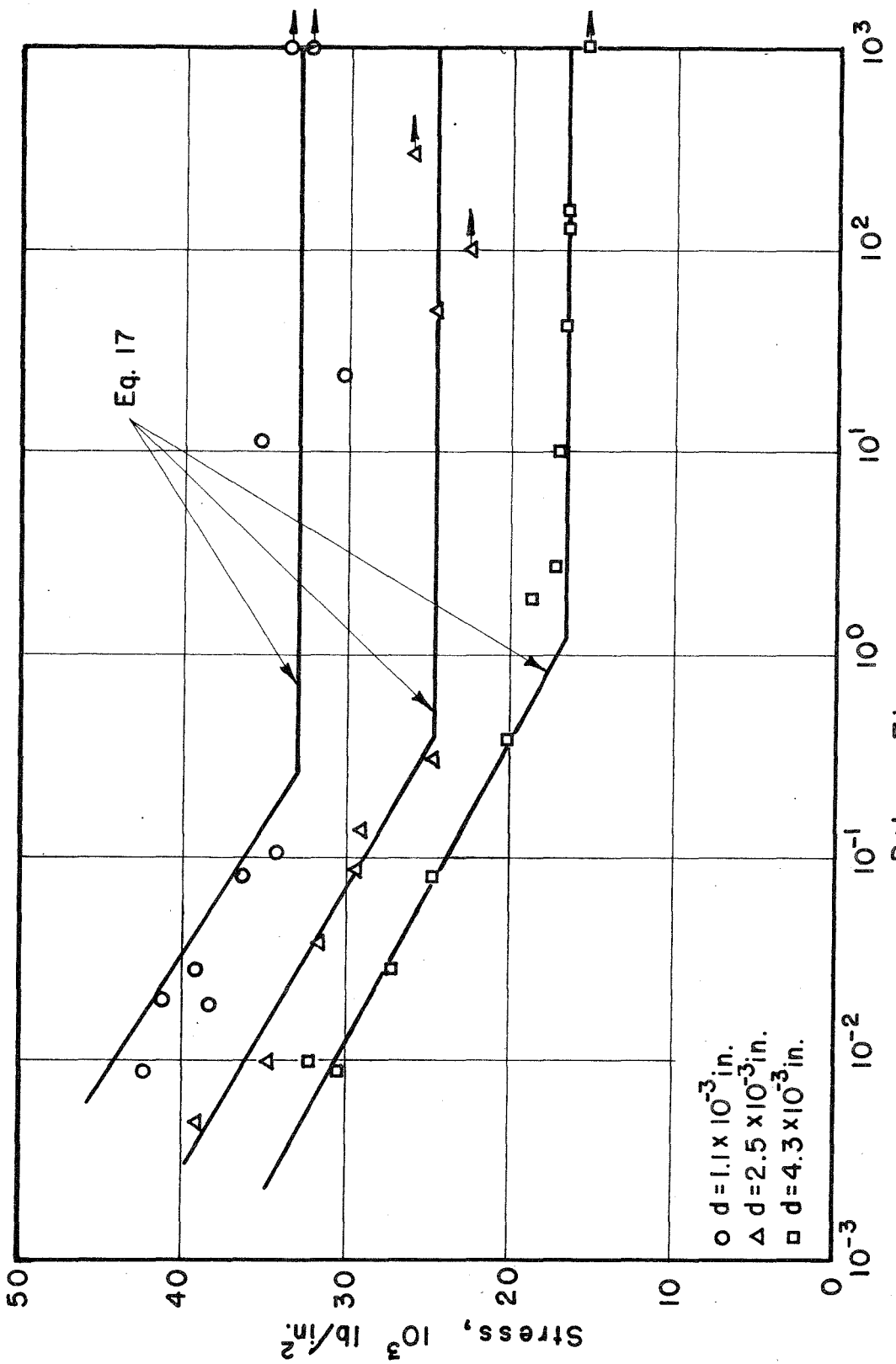

Fig. 19 Delay Time vs. Stress for Different Grain Sizes.

obtained from the specimens of the three smallest grain sizes are plotted, since the specimens of $d \geq 5.5 \times 10^{-3}$ in. did not exhibit a very strong static yield point or a distinct delay time. The general trend of all the data and the values of delay time for the specimens of the smallest grain size are in good agreement with similar measurements reported by Wood and Clark (2), (4).

The delay time decreases with increasing stress above a minimum value. This minimum stress, represented by the horizontal lines in figure 19, can be interpreted to be the stress below which yielding will never occur, even after a very long time. The effect of grain size on delay time is clear from figure 19. The delay time decreases at a given stress level, as the grain size is increased.

The minimum stresses measured in the rapid loading tests which will produce yielding in the three grain sizes, shown as horizontal lines in figure 19, are approximately equal to the static upper yield points for specimens of these grain sizes. The results of the rapid loading tests strongly indicate that no yielding will occur if a specimen is subjected to a stress below the static upper yield point and above the static lower yield point.

The static tests on the two specimens of the largest grain sizes resulted in no yield point for $d = 8.1 \times 10^{-3}$ in. and only a weak yield point for $d = 5.5 \times 10^{-3}$ in. The rapid loading tests on the specimens of these two grain sizes resulted in strain-time history which did not exhibit a delay time.

This comparison of the results of the static and rapid loading tests indicates good agreement between the yielding behavior observed under static and rapid loading conditions. In addition these

results support the theory that the upper and lower yield points are separate and distinct phenomena.

Fisher (8) has derived an expression for delay time as a function of stress and temperature by a quantitative treatment of Cottrell's mechanism for yielding. To make this calculation Fisher has greatly simplified the expression of Cottrell and Bilby (11) for the energy necessary to release a dislocation from an atmosphere. Fisher, in his treatment, assumed that yielding occurred when a given number of dislocations had been generated.

Fisher's treatment of Cottrell's mechanism assumes that a source can only generate a dislocation with the aid of a thermal fluctuation in the lattice. Therefore the delay time is related to the frequency and magnitude of thermal fluctuations which are able to free a dislocation segment from an "atmosphere" of carbon atoms. Fisher calculated the energy necessary to free a dislocation from the influence of its carbon atmosphere, by assuming that the activated dislocation segment consists of a circular arc. By using this energy as the energy to be supplied by a thermal excitation of the lattice, the delay time can be expressed as

$$t_d = \frac{n_y}{n_s \nu} e^{W/KT} \qquad (11)$$

where n_y = the critical number of dislocation rings which will cause yielding

n_s = the number of possible sites for active sources

ν = a frequency factor for the appropriate thermal fluctuations

W = the thermal energy necessary to release a

dislocation from a source

K = Boltzman's constant

T = absolute temperature.

The energy, W, to be supplied thermally is given by

$$W = \frac{\gamma_o^2}{b\tau} f\left(\frac{\gamma}{\gamma_o}\right) \tag{12}$$

where $f\left(\frac{\gamma}{\gamma_o}\right) = \cos^{-1}\left(\frac{\gamma}{\gamma_o}\right) - \frac{\gamma}{\gamma_o}\left(1-\frac{\gamma^2}{\gamma_o^2}\right)^{\frac{1}{2}}$

γ_o = the energy per atomic distance of a dislocation without an "atmosphere"

γ = the energy per atomic distance of a dislocation with an "atmosphere"

b = the atomic slip distance or Burgers vector

τ = the resolved shear stress in the slip plane.

Fisher has fitted this expression to the experimental results of Clark and Wood (2), (5), in which delay time as a function of both stress and temperature are reported. After fitting the expression for delay time, Fisher has obtained a numerical value for the ratio of the binding energy between a dislocation and its atmosphere to the energy of a free dislocation, $\left(1-\frac{\gamma}{\gamma_o}\right)$. The value of $\left(1-\frac{\gamma}{\gamma_o}\right)$ obtained in this way equals approximately 1/3 of one per cent. This value is in contrast to approximately 10 per cent estimated by Cottrell (23).

Fisher's expression for delay time is not a function of grain size. Therefore this treatment of Cottrell's mechanism gives a delay time that is independent of the grain size of the material tested. This result is in sharp disagreement with the experimental results of this

investigation.

Vreeland and Wood (9) have proposed several modifications to Fisher's treatment. Fundamentally the same calculations have been made by Vreeland and Wood, but two refinements have been added. First, the criterion for propagation of slip in successive grains is assumed to be a critical stress occurring at a grain boundary. Fisher's original criterion for yielding was that a critical number of dislocations had to be generated. The results of the static tests of this investigation give greater support to the yield criteria assumed by Vreeland and Wood in their treatment. Second, the net stress acting on a Frank-Read source is not taken to be constant and equal to the applied shear stress. Instead Vreeland and Wood took the stress at the source to be a decreasing function of the number of dislocation rings generated. With these refinements to Fisher's treatment, Vreeland and Wood calculated a more complex expression for delay time.

$$t_d = \frac{1}{D}\int_0^{n=\frac{\tau_b^*}{\tau}} \exp\left[\frac{\gamma_o^2 f\left(\frac{\gamma}{\gamma_o}\right)}{\tau b K T\left(1-\frac{n\pi B}{\tau L}\right)^{\frac{1}{2}}}\right] dn \qquad (13)$$

where τ_b^* = the critical stress at the head of a pile-up which will cause slip in successive grains

$B = \frac{Gb}{2\pi}$

L = one half the shortest distance in a slip plane from source to grain boundary.

Vreeland and Wood have shown that this expression can also be fitted to the delay time data of Wood and Clark. However, these refinements make no change in the value of $\left(1-\frac{\gamma}{\gamma_o}\right)$ originally obtained by Fisher.

Vreeland and Wood's expression for delay time given in equation 13 does exhibit a dependence on grain size. L is a function of grain size, such that 2L is proportional to d. However, this expression for delay time is not adequate to explain the observed influence of grain size. Upon further examination of Vreeland and Wood's expression for delay time it can be shown that the factor containing L in equation 13 is only a second order correction term. Consequently changes in L due to changes in grain size do not markedly influence the delay time. Hence, Vreeland and Wood's refinements to Fisher's treatment are not sufficient to account for the observed influence of grain size.

Cottrell (12) has recently proposed a new approach for the quantitative treatment of his general mechanism for the initiation of yielding. In this treatment a segment of a dislocation source only a few atomic spacings long is assumed to initially free itself from the influence of the carbon atmosphere. This dislocation segment is assumed to take the form of a small square. Only the interaction between the carbon atmosphere and the segment of the dislocation making up the side of the square parallel to the source is considered. In his treatment the energy is calculated from an assumed relationship for the interaction stress between a dislocation and an atmosphere as a function of the distance between them. After calculating this energy, Cottrell expresses the delay time as

$$t_d = t_0 e^{U(r/r_0)/kT} \qquad (14)$$

where $$U(r/r_0) = 9 r_0 b^3 \left(1 - \frac{r}{r_0}\right)^3$$

τ_o = the shear stress required to free a dislocation from an "atmosphere" at absolute zero

t_o = a factor proportional to the frequency of thermal fluctuations.

Cottrell has shown that equation 14 can be fitted to the experimental data of Wood and Clark in which delay time is reported as a function of stress and temperature. The value of τ_o obtained by this procedure is shown by Cottrell to be in good agreement with other theoretical and experimental results.

The expression for delay time resulting from Cottrell's treatment is independent of grain size. Additional refinements such as Vreeland and Wood suggested for Fisher's analysis could be applied. But, again, these refinements would not appear to solve the problem of calculating an expression for delay time which will explain the influence of grain size observed in this investigation.

An expression for delay time that is a function of grain size can be derived by making several modifications of Cottrell's mechanism for yielding. The new model for yielding that is to be presented here is basically very similar to Cottrell's, the major differences resulting only from the addition of certain refinements.

The criterion for yielding in this model is taken to be that some fraction of the total number of grains in the specimen must contain at least one pile-up of enough dislocations to produce a critical stress equal to τ_b^* at a grain boundary. Thus the conditions for yielding to occur not only require a critical stress at a point in a grain boundary but also require that this stress occur in a critical number of grains. Further, it will be assumed that when a pile-up in a grain

has been generated, any other sources present in that grain will not generate a large number of additional dislocations. The activation of one source will tend to relax the stress in the grain, thereby reducing the probability of the activation of any other sources in that grain.

Fisher, Hart and Pry (17) have proposed that a Frank-Read source will generate dislocation rings in bursts instead of individually. The number of dislocations in each burst will be determined by how rapidly the back stress due to the generated dislocations is built up at the source, since there is a minimum stress at which a source will stop generating. Another burst will only be generated when the first burst has moved away and when a second thermal fluctuation of sufficient magnitude to activate the source occurs.

With the addition of these refinements to Cottrell's mechanism and using his expression for the thermal activation energy required to liberate a dislocation from its source, an expression for delay time may be calculated.

The rate at which dislocation pile-ups capable of exerting a stress equal to τ_b^* at a grain boundary will be formed, if only one pile-up per grain can occur, is given by

$$\dot{N} = (N_o - N)\frac{n_1}{n^*}\rho d^3 \nu e^{-U/KT} \qquad (15)$$

where $$U = \vartheta \tau_o b^3 \left(1 - \frac{\tau}{\tau_o}\right)^3$$

N = the number of grains per unit volume containing a pile-up of n^* dislocations

N_o = the total number of grains per unit volume

n_1 = the number of dislocations generated in one burst

n^* = the number of dislocations in a pile-up required to produce a stress equal to τ_b^*

ρ = the density of sources that can be thermally activated

d = the average grain diameter.

From the integration of equation 15 the time to produce pile-ups of n^* dislocations in N/N_o grains is

$$t = \frac{n^* \ln\left(\frac{1}{1-m}\right)}{\rho d^3 \nu n_1} e^{U/KT} \tag{16}$$

where $m = \frac{N}{N_o}$ fraction of the total number of grains which contain critical pile-ups.

From Eshelby, Frank, and Nabarro's expression for the stress at the front of a dislocation pile-up τ_b^*/τ can be substituted for n^*. When the fraction of the grains containing a critical pile-up, m, reaches a critical number denoted by m^* yielding will occur. If m^* is small compared to one, then equation 16 may be rewritten

$$t_d = \frac{Z}{d^3 \tau} e^{U/KT} \tag{17}$$

where $Z = \frac{\tau_b^* m^*}{\rho \nu n_1}$ and $U = 9 \tau_o b^3 \left(1 - \frac{\tau}{\tau_o}\right)^3$.

This expression for delay time may be fitted to the experimental data of this investigation by choosing appropriate values for the two constants Z and τ_o. The delay times calculated from equation 17, with $Z = 1.10 \times 10^{-16}$ sec lb in. and $\tau_o = 1.5 \times 10^5$ lb/in^2. are shown in figure 19 as solid lines.

This value of τ_o resulting from the experimental data is equal to the value Cottrell used in fitting his original expression for delay time (equation 14) to Wood and Clark's experimental data. $\tau_o = 1.5 \times 10^5 \text{ lb/in}^2$ is of the proper order and Cottrell (12) shows that it compares favorably with results of other analytical and experimental investigations.

A theoretical value of the constant z cannot be calculated exactly because the parameters which it contains are unknown. However, by making estimates of $\rho, \upsilon, m^*, \tau_b^*$ and using the experimental value of z the order of n, may be estimated.

To estimate the frequency factor, υ, the segment of a source that is activated is assumed to be 4b long. Taking this length as approximately one half the wave length of a thermal fluctuation in the lattice gives $\upsilon = 3 \times 10^{12} \text{ sec}^{-1}$.

τ_b^* is approximately equal to $1 \times 10^6 \text{ lb/in}^2$. This value of the critical stress at the grain boundary was determined from the results of the static tests of this investigation.

m^* can be very roughly estimated from the observed values of microstrain which occur at yielding. The average shear strain in a grain containing one pile-up of n^* dislocations is approximately n^*b/d. Therefore the average shear strain, γ, over the whole specimen at yielding can be estimated to be

$$\gamma \cong \frac{n^* b}{d} m^* \qquad (18)$$

For the specimens of the smallest grain size, taking $d \cong 1 \times 10^{-3}$ in., $b \cong 10^{-8}$ in., and $n^* = \frac{\tau_b^*}{\tau_y} \cong 10^2$ gives $\frac{n^* b}{d} \cong 10^{-3}$ in. The observed tensile strain at yielding in the specimens of the smallest grain size is of the order of 50×10^{-6} in./in. Letting $\varepsilon \cong \frac{1}{2} \gamma$, where ε = the tensile strain, gives $m^* \cong \frac{1}{10}$. This means

that at yielding only about a tenth of the grains will contain dislocation pile-ups of n^* dislocations.

The order of magnitude of ρ can also be estimated. In the specimens of the smallest grain size the value of equilibrium microstrain after rapid loading to a stress just below the static yield point is approximately equal to the value of microstrain observed at yielding. Therefore, ρ must have a value which gives approximately the same number of potential dislocation sources per grain as the number implied by the value of m^*. If ρ gives a total number of sources larger than the number given by m^* then the amount of equilibrium microstrain just below the yield point would be much larger than the amount of microstrain occurring at yielding. Thus in the smallest grain size if ρ gives one source for every 10 grains then ρ will equal approximately 7×10^7 in^{-3}. Substituting these estimated values for ν, τ_b^*, m^*, ρ, and the value of Z, determined by fitting the expression for delay time to the experimental data into the expression for Z, gives the number of dislocations per burst, $n_1 \cong 4$. This value for the number of dislocations in a burst is only a very rough estimate, but it is certainly of a reasonable order of magnitude. This determination of n_1 gives a value that is considerably smaller than the estimate of several hundred made by Fisher, Hart, and Pry (17). However, Fisher, Hart, and Pry's treatment also resulted in only a very rough estimate of this number.

Taking $\rho = 7 \times 10^7$ in^{-3}. as a constant independent of grain size will give one source per grain and 5 sources per grain in the specimens of d = 2.4×10^{-3} in. and 4.5×10^{-3} in. respectively. If m^*

remains 1/10 for these grain sizes, then one would expect the amount of equilibrium microstrain in rapid loading tests at stresses just below the static yield point to be very much greater than the microstrain at yielding. This behavior was not observed in the tests made during this investigation. Actually the value of ρ may be less in larger grained steel because the density of sources is not a constant independent of stress. The sources within a material are of varying lengths. The sources that can be activated are those whose length is greater than Gb/τ. If the applied stress is decreased, the number of active sources will decrease because the sources of shorter length will no longer be able to generate dislocations. Thus the value of ρ estimated for the specimens of small grain size may be decreased when the behavior of the specimens of larger grain sizes are being considered, because the applied stress at the yield point is smaller.

The previous treatments by Fisher, Vreeland and Wood, and Cottrell have implied that the yielding process is the result of a critical pile-up in one grain. In contrast to this fact, the present treatment involves the occurrence of critical pile-ups in some fraction of the total number of grains.

This treatment of Cottrell's yielding mechanism is also compatible with the results of the static tests. In a static test there may be, after a long time, more than m^* of the grains which contain pile-ups. However, the second criteria for yielding must also be satisfied, namely, τ_b^* must be produced at the grain boundary. Therefore, the static yield point is governed by a critical stress at the front of a dislocation pile-up in accord with the previous analysis of the static test data.

The assumptions and estimates made in the present treatment are numerous and very approximate. However, this treatment does offer several suggestions for improvements on the previous attempts to analyze Cottrell's yielding mechanism. Basically only three modifications to Cottrell's model have been made, namely: 1) There must be a critical number of dislocation pile-ups, each producing a critical stress at a grain boundary, in order to initiate yielding; 2) Frank-Read sources generate dislocations in bursts; 3) A pile-up of n^* dislocations relaxes the stress in the grain to the point that other sources are inactive. With these modifications, Cottrell's mechanism for yielding in a low-carbon steel explains the experimental observations of yielding behavior made in this investigation.

Plastic deformation by twinning was observed in the tensile tests performed at a temperature of -320°F. The results of these tests were summarized in Table V. The stress at which twinning is initiated was determined by rapid loading tests, static tests, and interrupted loading tests on specimens of all five grain sizes.

The results of the tests conducted at -320°F are plotted in figure 20, where the stress at which twinning occurs is plotted as a function of $d^{-1/2}$. The twinning stress is an increasing linear function of $d^{-1/2}$.

The specimens of the four larger grain sizes either twinned or did not plastically deform an observable amount when tested under rapid loading conditions. The initial plastic strain measured in these tests increased to values of 300 to 1000 x 10^{-6} in./in. within a time period of the order of 10^{-3} sec. There was no measurable

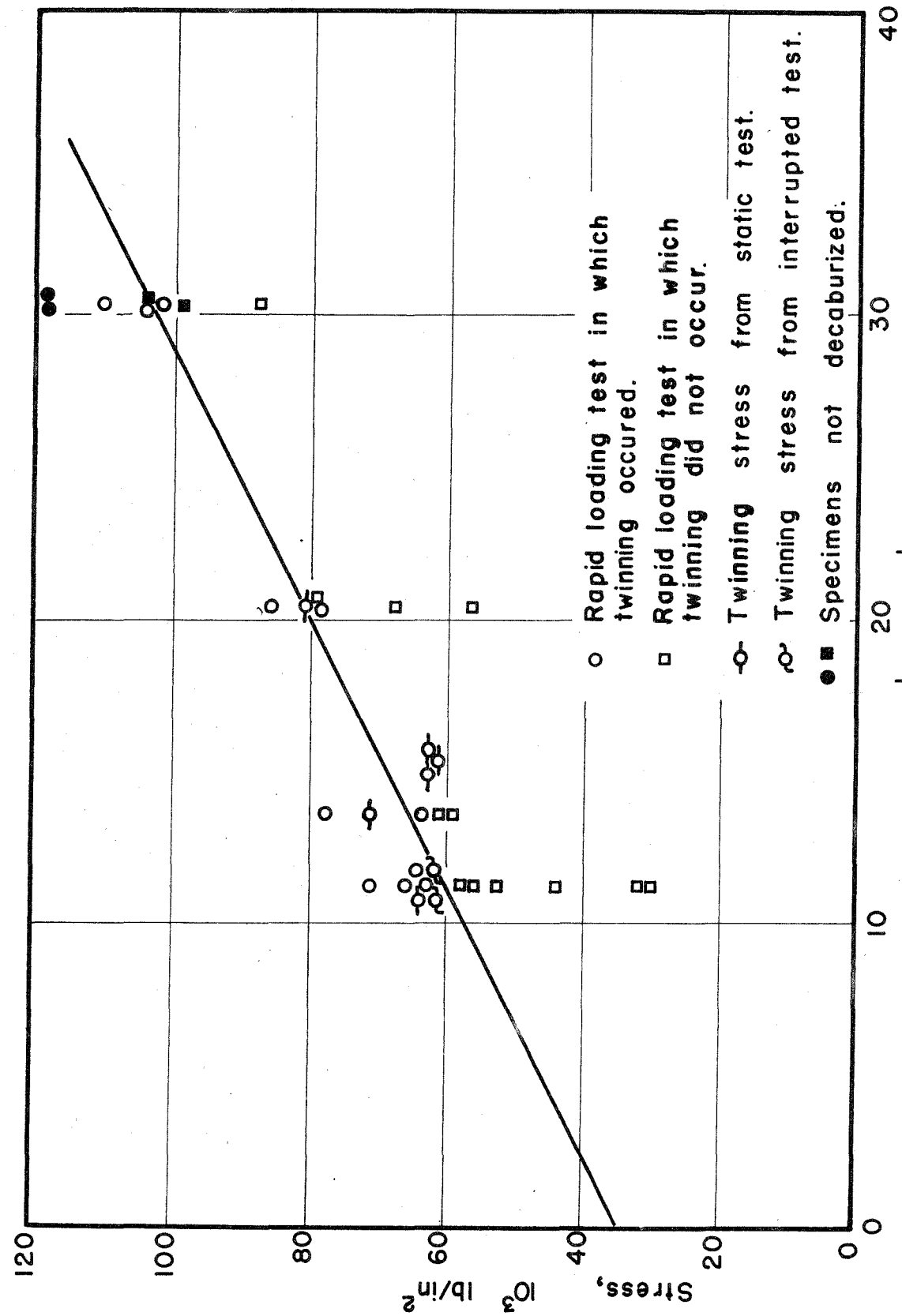

Fig. 20 Twinning Stress vs. Inverse Square Root of Average Grain Diameter.

plastic deformation in tests performed at stresses less than the critical value at which twinning occurred. The strain sensitivity is the order of 10×10^{-6} in./in. under the conditions imposed by low temperature tests.

Twinning stresses could be determined quite accurately from the results of the static and interrupted tests. The occurrence of twinning was indicated by an immediate increase in strain up to values as high as 1000×10^{-6} in./in. within a time of the order of 10^{-3} sec. There was no measurable plastic deformation before the occurrence of twinning. The twinning stresses resulting from static loading tests were very close to those deduced from the rapid loading tests. Hence one may conclude that there is a critical stress for twinning that is independent of loading rate over the range 10^{7} lb/in^2. sec to 500 lb/in^2. sec at -320°F.

The interrupted tests were performed in order to determine if the twinning stress could be increased by "aging" the specimen at -320°F at a stress just less than the normal twinning stress. There was no observable increase in the critical stress for twinning.

The existence of a critical stress for twinning is in agreement with results of tensile tests on single crystals reported by Cox, Horne, and Mehl (24). The value of the tensile stress to produce twinning in single crystals ($d^{-1/2} = 0$) extrapolated from the plot in figure 20 is $3.4 \times 10^{+4}$ lb/in^2. This value agrees with the results of Cox et al., who reported a shear stress of 1.4×10^{4} lb/in^2., to produce twinning in single crystals of iron.

Cottrell and Bilby (25) have suggested a dislocation mechanism

for the growth of a twin band by the motion of a single dislocation in a body-centered cubic structure. An analysis of this mechanism can explain the presence of a threshold stress for twinning in single crystals, thereby explaining the observations of Cox, Horne, and Mehl and of this investigation. However, Cottrell and Bilby's model alone is not sufficient to explain the dependence of the twinning stress on grain size.

Cottrell and Bilby visualized the formation of twinning deformation in the <111> direction of the $\{112\}$ planes by the dissociation of a slip dislocation. Under the action of a suitable shear stress a slip dislocation with a Burgers vector $a/2\ [111]$ lying in a (112) plane will dissociate into two dislocations. This is represented by the relation

$$\frac{a}{2}[111] \longrightarrow \frac{a}{3}[112] + \frac{a}{6}[11\bar{1}] \qquad (19)$$

The dislocation, $a/6\ [11\bar{1}]$, is mobile in twinning planes of the $\{112\}$ type and produces a twinning displacement in these planes. Under the action of a suitable applied stress, this twinning dislocation is free to move in the set of $\{112\}$ planes that are deformed into a helix by the remaining sessile partial dislocation, $a/3\ [112]$. Consequently the twinning dislocation rotating about one end in the helical surface of a $\{112\}$ set of planes can climb through the lattice thereby producing a band of twinned material.

Figure 21 shows the twinning and sessile partial dislocations after they have separated a short distance. The plane of the figure is $(1\bar{1}0)$. The atmosphere of carbon and/or nitrogen atoms associated

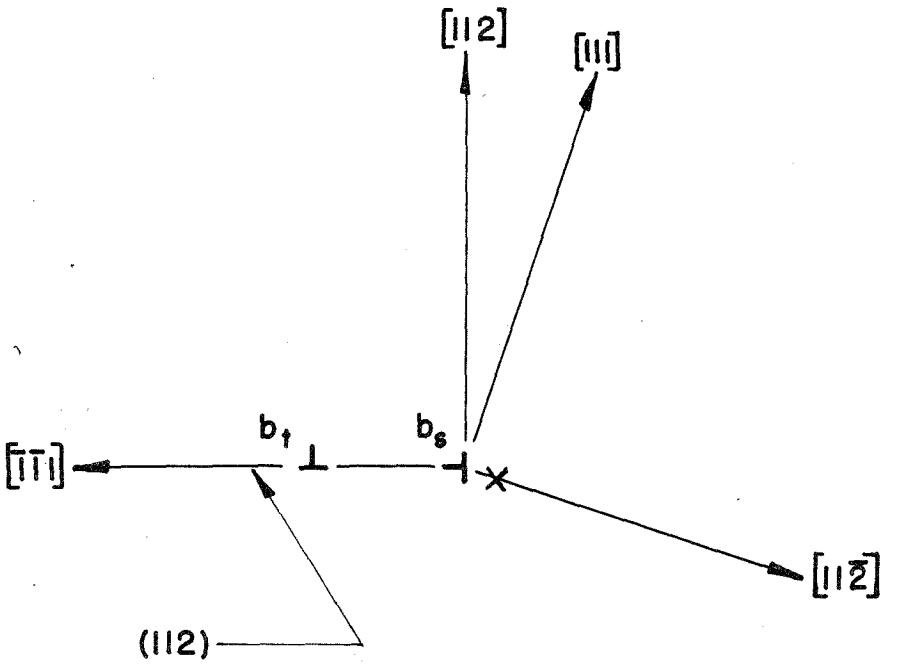

Fig. 21 Schematic Representation of Twin and Sessile Dislocations after Dissociation of a Slip Dislocation.

$b_s = \frac{a}{2}[112]$ = Burgers Vector of Sessile Partial Dislocation.

$b_t = \frac{a}{6}[11\bar{1}]$ = Burgers Vector of Twinning Dislocation.

x = Position of the "Atmosphere".

with the original slip dislocation, a/2 [111] is indicated by x in the figure.

The release of the twinning dislocation from the atmosphere under the combined action of an applied shear stress and thermal fluctuations may be analyzed in the following manner: Before a segment of the twinning dislocation can expand in the twinning plane, the stress must be of sufficient magnitude to supply the stacking fault energy resulting from the motion of the twinning dislocation. If a segment of a twinning dislocation is to expand, then

$$\tau b_t > f \tag{20}$$

where τ = the applied resolved shear stress

b_t = Burgers vector for the twinning dislocation

f = the stacking fault energy per unit area.

Therefore the minimum stress, τ_t , at which twinning can occur is given by

$$\tau_t = \frac{f}{b_t} \tag{21}$$

If the liberation of a twinning dislocation from a carbon atmosphere requires less thermal energy than the release of a slip dislocation at a stress equal to τ_t , then twinning dislocations will be generated at a faster rate than slip dislocations. Therefore τ_t will be the critical stress for twinning.

The relative rates of generation of twin dislocations and of slip dislocations can be calculated for a stress equal to the twinning stress. The thermal energy, derived by Cottrell, to release a slip dislocation from a source is given by equation 15. The thermal energy to release

a twinning dislocation is given by

$$U_t = 9\tau_o b_t^3 \left(1 - \frac{\tau}{\tau_o}\right)^3 \qquad (22)$$

The ratio of the generation rates of twinning dislocations to slip dislocations is

$$\frac{\dot{N}_t}{\dot{N}_s} = e^{(U-U_t)/KT} \qquad (23)$$

where $\dot{N}_t$ = rate of generation of twinning dislocations

$\dot{N}_s$ = rate of generation of slip dislocations.

Substituting $b_t = \frac{b}{3}$, $\tau_o = 1.5 \times 10^5$ lb/in^2., $\tau_t = 1.7 \times 10^4$ lb/in^2., and $b = 0.985 \times 10^{-8}$ into equation 23 gives

$$\frac{\dot{N}_t}{\dot{N}_s} = e^{95}$$

Therefore when the applied stress increases to the stress at which twinning can occur, the release of twinning dislocations is very much more probable than the release of slip dislocations. Hence, there will be a critical stress given by $\tau_t = \gamma/b_t$ at which twinning will occur.

Taking the twinning stress for a single crystal ($d^{-1/2} = 0$) to be 1.7×10^4 lb/in^2. and solving for the stacking fault energy gives $\gamma = 9.8$ ergs/cm^2. Although the stacking fault energy for body-centered cubic iron has not been measured, this value certainly compares favorably with the order of magnitude of the twin boundary energies reported for other metals.

This treatment of Cottrell's mechanism does not account for the increase of twinning stress with decreasing grain size. This

behavior must be investigated further. Perhaps a mechanism which included some hindrance to dislocation motion, such as that postulated in the yielding mechanism, would solve this difficulty.

The twinning stress observed in this investigation is larger than the stress required to produce slip at room temperature. If the twinning stress is fairly insensitive to temperature, the material cannot reach the twinning stress at room temperature without large amounts of slip occurring first. Severe slip will reduce the likelihood of twin formation, even when the stress increases to the critical value for twin formation. This effect can be explained in terms of the treatment presented here by the fact that after considerable slipping has occurred, the active dislocation sources are exhausted. In addition, the dislocation density in the material will be greatly increased, thereby making it much harder for a twin dislocation to move through the lattice. Only with very high stress rates or at low temperatures can the twinning stress be attained without excessive slip taking place at a lower stress. Thus twinning will occur only at low temperatures or high stress rates. This conclusion is in good agreement with experimental observations. The occurrence of twinning in iron or steel is usually limited to tests performed at low temperatures, of the order of $77^{\circ}K$ or below, except when the loading rates are extremely high, such as in impact tests, in the region of a fast moving crack, or under explosive loading conditions.

The exact mechanism for the initiation of twinning is certainly not clear. However, from the results reported here, some of the factors which influence this phenomenon can be better understood,

leaving the way clear for further experimental and theoretical investigations. In particular, some addition must be made to Cottrell's mechanism if the dependence of the twinning stress upon grain size is to be understood.

VI. SUMMARY AND CONCLUSION

The results of the static tests on specimens of different grain sizes are consistent with the theory that both the upper and lower yield points are an increasing linear function of $d^{-1/2}$, where d is the average grain diameter. There is no yield point for specimens of a grain size larger than a critical diameter. This behavior of the yield point as a function of grain size has been shown to be the result of dislocations piling up at an obstacle. The upper yield point results from a dislocation pile-up breaking through a grain boundary. The lower yield point is the stress required to form dislocation pile-ups of sufficient strength to overcome the resistance to motion resulting from collision with other dislocation arrays.

The measurement of plastic strain during rapid loading of specimens of different grain sizes indicates that a delay time can only be observed in low-carbon steels of a grain size small enough to exhibit a pronounced static yield point. The results of rapid loading tests on specimens which exhibited a yield point show that the delay time decreases with increasing grain size for a given stress. The author has presented a dislocation model similar to Cottrell's mechanism for yielding, but with several refinements. This model is consistent with the experimental measurements of this investigation. The refinements are: 1) A critical number of dislocation pile-ups of sufficient strength to cause a critical stress at a grain boundary is taken to be the criterion for yielding: 2) Frank-Read sources generate bursts of dislocations when activated by a single thermal fluctuation: 3) After one Frank-Read source has been activated in a given grain, all other sources in that grain are inactive because of the back stress produced by the dislocation

array generated from the first source.

Plastic deformation by twinning is observed to be initiated by a critical stress. The value of the twinning stress increases with decreasing grain size. The theory of Cottrell is shown to explain the existence of a critical stress for twinning in a single crystal. Cottrell's theory does not account for the increase in twinning stress with decreasing grain size.

It is suggested that the yielding of low-carbon steels be further studied with the use of etching techniques to attempt the direct observation of dislocations at various stages of the yielding process. Better information concerning the position of dislocations during the yielding process is needed before a detailed model for yielding can be definitely confirmed.

APPENDIX A

DISCUSSION OF GRAIN SIZE DISTRIBUTION

The measurement of the grain size of a metal presents a complicated problem. The grain size may be reported in terms of several parameters. Some of these parameters are:

1) The average linear distance between grain boundaries along a straight line drawn at random through the structure.
2) The average grain area enclosed by grain boundaries on a random plane through the structure.
3) Grain diameter given by the square root of the average grain area on a random plane.
4) The average volume of the grains.
5) The average grain diameter obtained by volumetric considerations.

In addition to the average value of these parameters, one may also be interested in their distribution about the average.

The choice of a parameter to describe gain size will, of course, depend on the purpose for which the measurement is made. However, to investigate the uniformity of grain size in a particular structure, a parameter based on volumetric considerations would seem to be logical because of the three dimensional character of grains. From practical considerations volume measurements are very difficult. Volumetric grain size relationships, while difficult to measure directly, may be estimated from other parameters. Since the grain area on a random plane is easily measured, the relationship between this area, or its diameter, and grain volume will be of help in estimating the uniformity of grain size.

The distribution of the diameters of grain areas observed on a plane intersecting a random array of equal volume spheres is given by the plot in figure A-1. This relationship is only a rough approximation to actual granular arrays since grains are certainly not spherical in shape. However, from this plot it is clear that equal volume grains would very likely result in a broad distribution of the diameters of grain areas observed on a random plane.

Hull and Houk (26) have shown experimentally that the distribution of "grain" diameters resulting from a plane intersecting an array of equal volume cubes, orthic tetrakaideckhedrons and pentagonal dodecahedrons are all similar and in addition do not vary a great deal from the distribution curve observed for spheres. The distribution curve for these shapes has a slightly higher value than the curve for spheres at small diameters. This distribution curve increases to a sharp maximum at a point between 85 and 95 per cent of the maximum "grain" diameter and then decreases to zero at 100 per cent. Even though metallic grains are not spheres or regular polyhedra, one should expect a similar distribution of grain diameters for an array of equal volume grains. Therefore, if the grain structure is truly uniform, the distribution curve of the diameters of grain areas measured on a plane should exhibit a maximum frequency at a fairly large grain diameter, with a larger percentage of the diameters falling in a range close to the most frequent diameter.

A technique for treating the problem of relating the diameter of grain areas observed on a plane to the true grain diameter of a three dimensional shape has been presented by Schiel (27). This

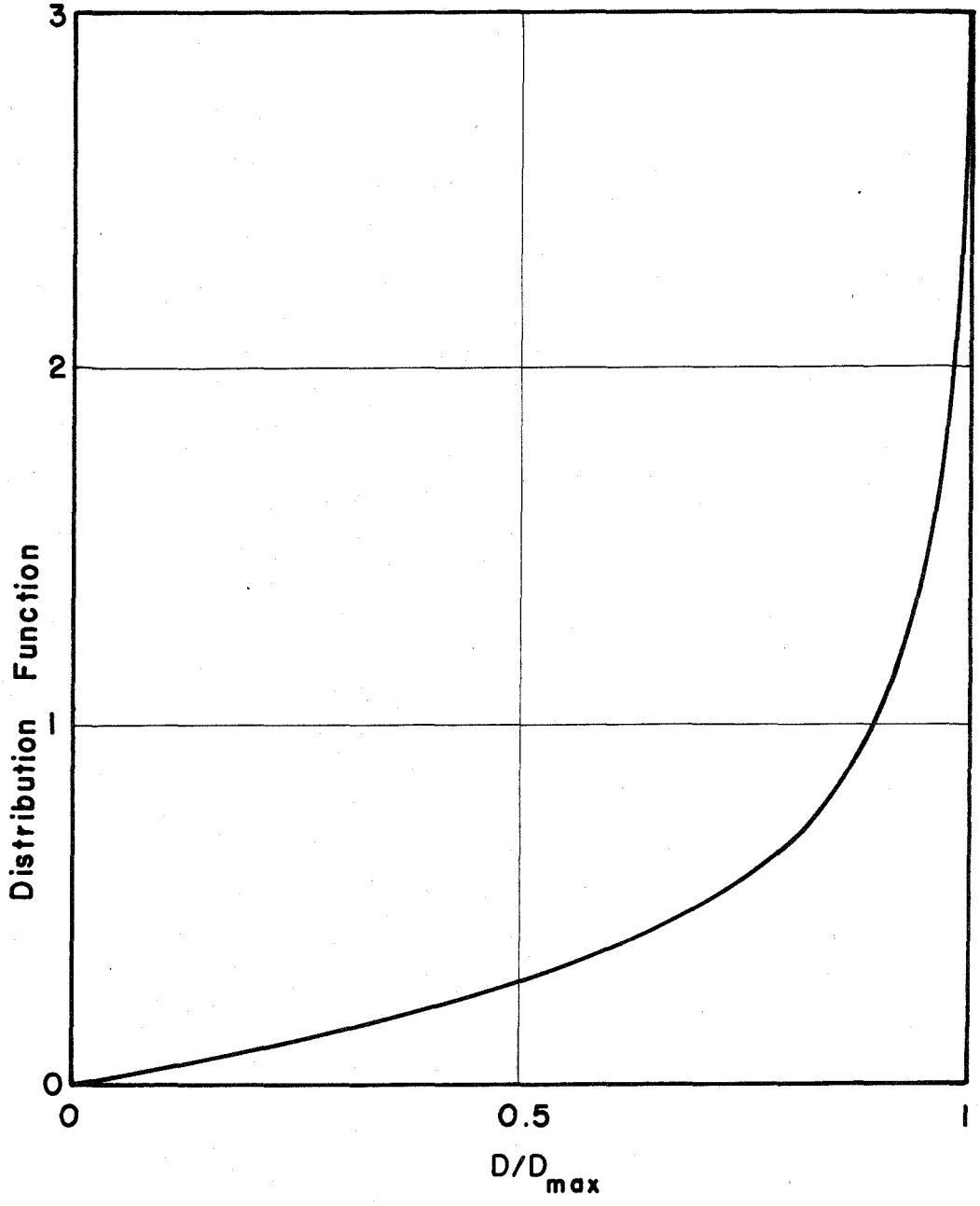

Fig. A-1 Distribution of the Diameter of "Grain" Areas Observed on a Random Plane Through Spheres Equal Volume.

treatment involves a statistical method for finding the distribution of the true grain diameters from the distribution of the diameters of grain areas measured on a random plane.

Distribution curves for the diameter of the grain areas on a random plane were determined for each grain size, in order to investigate the uniformity of the grain structures. The areas of the grains on an intersecting plane were determined from photomicrographs, by overlaying a plastic sheet containing a series of circular holes of various diameters. The area of a hole and a grain were then matched by eye. The diameter of the hole making the closest fit was recorded as the grain diameter. Typical distribution curves for four recrystallized grain structures are shown in figure A-2. The diameter of the average areas reported in figure A-2 were computed by counting the grains appearing in a given area of the microstructure.

Distributions of true grain diameter were computed by Schiel's technique, from the distribution of the diameters of grain areas measured on a random plane. A typical result of these calculations are shown in figure A-3.

The observed distributions of grain diameter presented in figure A-2 is not the distribution one would expect for uniform grains. This fact, coupled with the results of the calculations of true grain diameter presented in figure A-3 strongly indicates that the grain structures produced for this investigation were not uniform.

Several techniques were investigated in the hope of producing grains of more nearly uniform volume. These techniques included:

1) Recrystallization at different temperatures for various times.

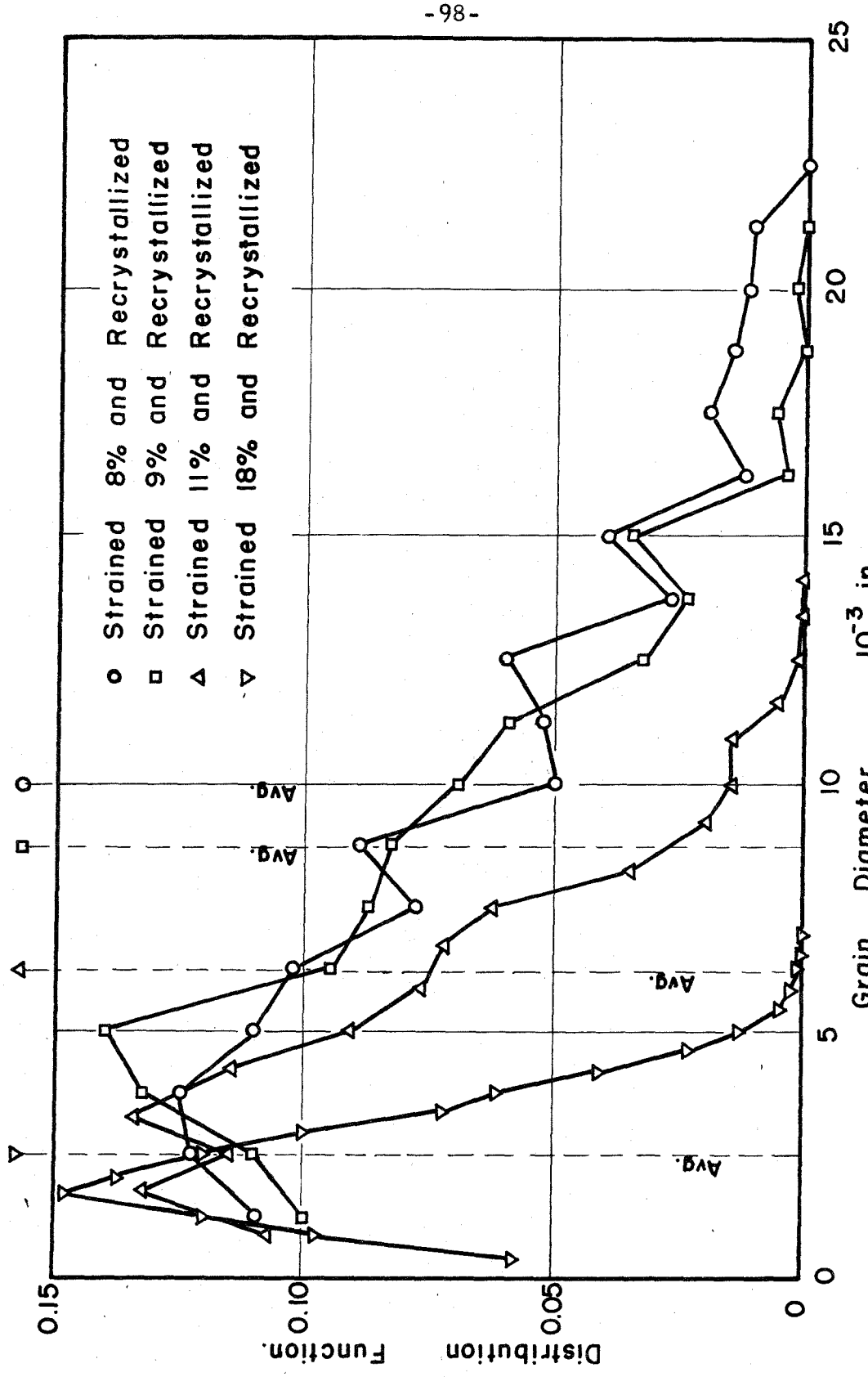

Fig. A-2 Observed Distribution of the Diameter of Grain Areas.

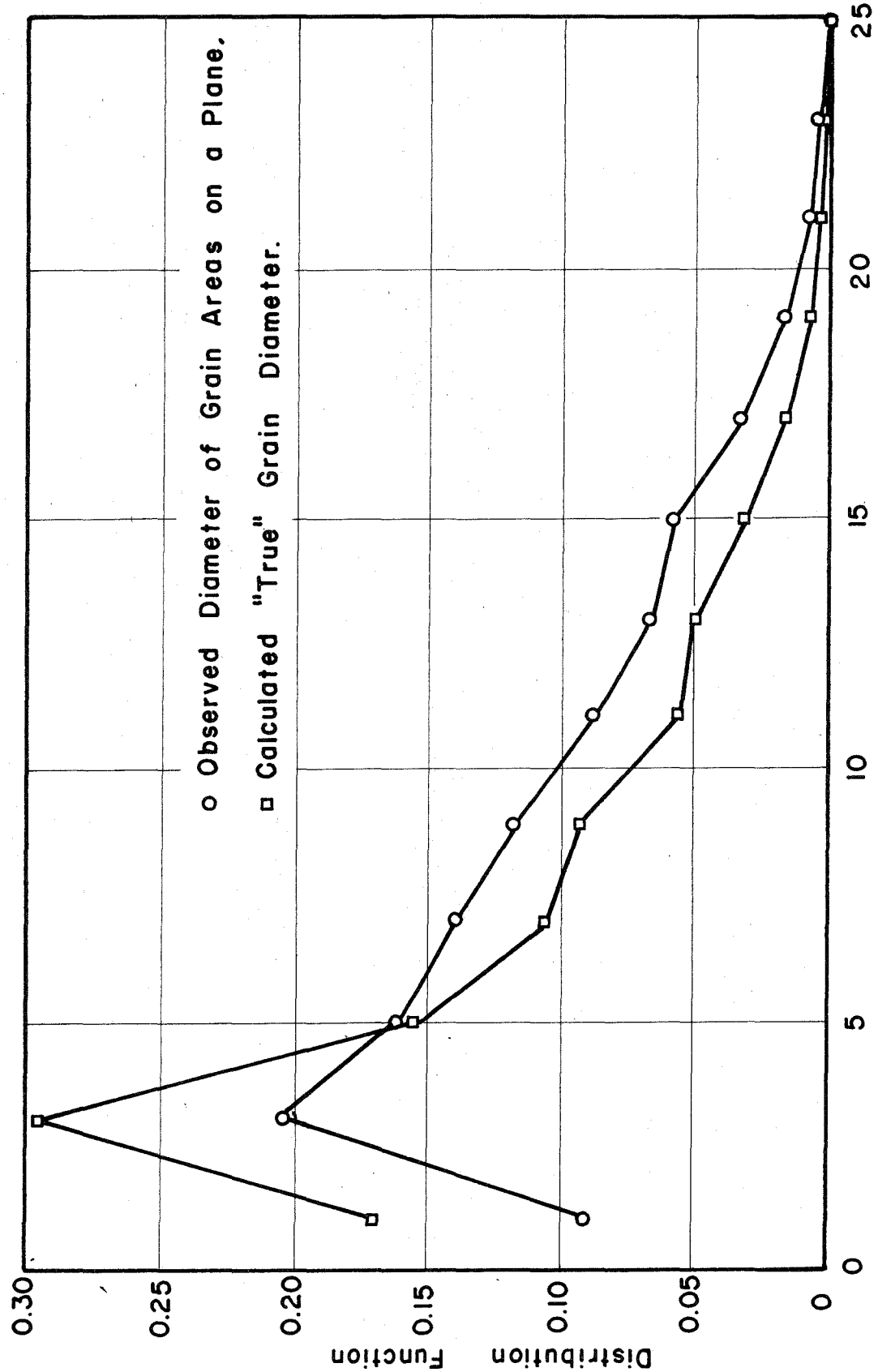

Fig. A-3 Distribution of the Diameter of Grain Areas and Distribution of "True" Grain Diameter.

2) Quenching from above the transformation temperature into water, followed by various tempering treatments.

3) Quenching from above the transformation temperature to various temperatures above room temperature.

A summary of these treatments is given in Table A-1. None of the treatments listed in Table A-1 produced a more uniform grain structure. The distribution curves obtained from these grain structures were all very similar to those shown in figure A-2. This study of the uniformity of grain size indicates that it may be very difficult to obtain a truly uniform grain size in a metal.

The distribution curves shown in figure A-3 indicate that the distribution of grain diameters based on grain volume are very similar to the distribution of the diameters of grain areas in a random plane. This fact coupled with Hull and Houk's observations indicate that the grain diameter derived from the area of grains on a plane, which is measured directly, is a fair indication of the grain diameter that would be obtained from volumetric considerations. The choice of average grain diameter to measure grain size can also be supported by the fact that in this investigation, the distance from a point in a slip plane to a grain boundary will be of interest. Since slip planes may be considered random planes, the distance from a point in this plane to the grain boundary is described best by some function of the diameter of a grain area measured on a random plane.

TABLE A-I

TREATMENTS INVESTIGATED TO OBTAIN A UNIFORM GRAIN SIZE

Recrystallization

Strain	Temperatures	Time at temperature
30%	1100, 1200, 1300°F	1, 5, 20, 50 hours
20%	1100, 1200, 1300°F	1, 5, 20, 50 hours
14%	1100, 1200, 1300°F	1, 5, 20, 50 hours
10%	1100, 1200, 1300°F	1, 5, 20, 50 hours
8%	1100, 1200, 1300°F	1, 5, 20, 50 hours

Water Quench and Temper

Temperature Quenched from	Tempering Temperature	Tempering Time
1700°F	800°F	2, 19, 71 hours
1700°F	1000°F	1, 4, 17, 40, 160 hours
1700°F	1300°F	1, 3, 18, 44, 114 hours

Quenching to Various Temperatures

1700°F	360°F	1 hour
1700°F	860°F	1 hour
1700°F	1350°F	8 hours
1650°F	1350°F	6 1/2, 8, 18 hours
1700°F	1300°F	5 sec, 5 min, 1, 6 hours

APPENDIX B

CALCULATION OF DISTANCE FROM DISLOCATION SOURCE TO GRAIN BOUNDARY

The average distance from randomly distributed dislocation sources to a grain boundary in a slip plane may be calculated if the grain is assumed to be spherical in shape and the density of sources is uniform throughout the grain.

The plane, shown in figure B-1, has a diameter equal to the average diameter, d_m, of all parallel slip planes in a grain of diameter d. The diameter d_1 is chosen so that the enclosed area contains one half of all sources in this average plane. The number of sources in a region of a plane will be proportional to the area of that region provided the sources are uniformly distributed. Therefore the area enclosed in the circle of diameter d_1 is equal to one half the area of the average plane. Under these conditions C represents the average distance from source to boundary in a slip plane of average diameter. This average distance, C, is given by

$$C = \frac{1}{2}\left(d_m - d_1\right) \tag{B-1}$$

where

$$d_m = 2\int_0^{d/2} \frac{\sqrt{\frac{d^2}{4} - z^2}}{\frac{d}{2}}\, dz = \frac{\pi d}{4} \tag{B-2}$$

and

$$d_1 = \frac{d_m}{\sqrt{2}} \tag{B-3}$$

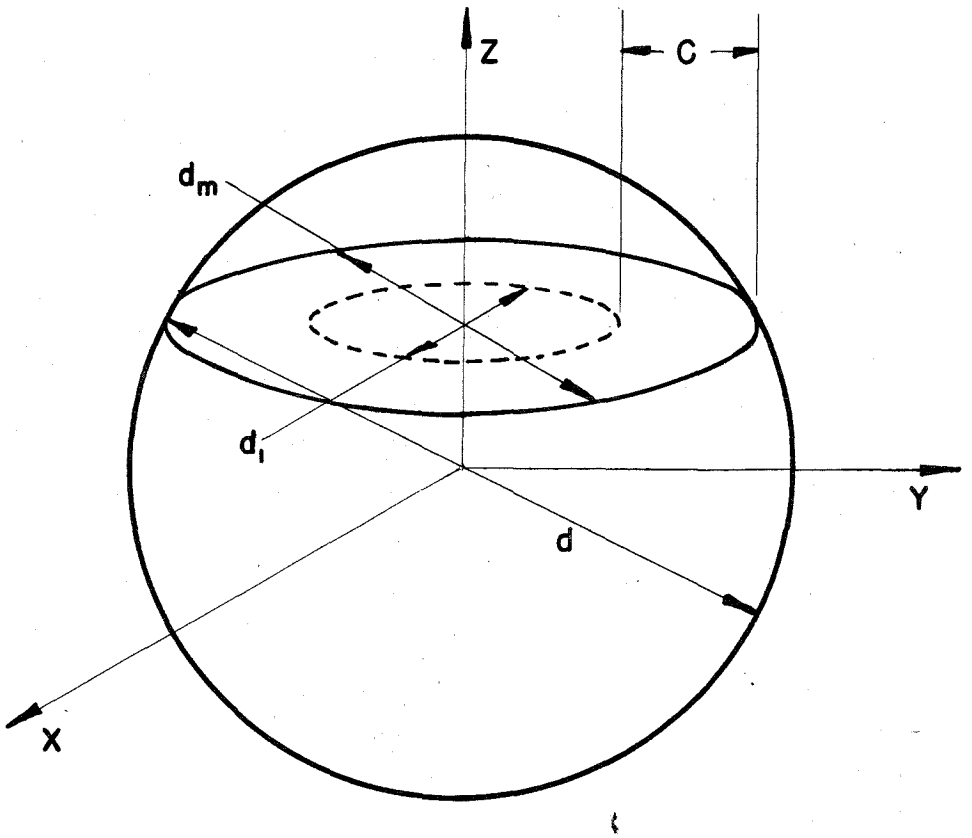

Fig. B-1 Schematic Representation of a Slip Plane in a Grain.

Combining equations B-1, B-2, and B-3 gives

$$C = \frac{\pi}{8}\left(1-\frac{1}{\sqrt{2}}\right)d$$

or

$$C = fd$$

where

$$f = \frac{\pi}{8}\left(1-\frac{1}{\sqrt{2}}\right) = 0.12.$$

REFERENCES

(1) J. R. Low, Jr. and M. Gensamer, "Aging and the Yield Point in Steel", Transactions of the American Institute of Mining and Metallurgical Engineers, (1944), Vol. 158, p. 207.

(2) D. S. Wood and D. S. Clark, "Delayed Yield in Annealed Steels of Very Low Carbon and Nitrogen Content", Transactions of the American Society for Metals, (1952), Vol. 44, p. 726.

(3) A. N. Holden and J. H. Holloman, "Homogeneous Yielding of Carburized and Nitrided Single Iron Crystals", Journal of Metals, Metals Transactions, (1949), Vol. 185, p. 179.

(4) D. S. Wood and D. S. Clark, "The Influence of Stress and Temperature on the Time for the Initiation of Plastic Deformation in an Annealed Low-Carbon Steel", Transactions of the American Society for Metals, (1951), Vol. 43, p. 571.

(5) D. S. Wood and D. S. Clark, "Delayed Yielding in Annealed Mild Steel with Special Reference to Yielding at Low Temperatures", Fourth Technical Report under Office of Naval Research, Contract N6 onr-24418, California Institute of Technology, (December 1951).

(6) T. Vreeland, Jr., D. S. Wood, and D. S. Clark, "Pre-Yield Plastic and Anelastic Microstrain in Low-Carbon Steel", Acta Metallurgica, (1953), Vol. 1, p. 414.

(7) H. Muir, B. L. Averbach, and M. Cohen, "The Elastic Limit and Yield Behavior of Hardened Steels", Transaction of the American Society for Metals, (1952), Vol. 47, p. 380.

(8) J. C. Fisher, "Application of Cottrell's Theory of Yielding to Delayed Yield in Steel", Transactions of the American Society for Metals, (1955), Vol. 47, p. 451.

REFERENCES (Cont'd)

(9) T. Vreeland, Jr. and D. S. Wood, "A Comparison Between Dislocation Theory and Experimental Measurements of Delayed Yield in Steel", Eighth Technical Report under Office of Naval Research, Contract N6 onr-24418, California Institute of Technology, (April 1954).

(10) A. H. Cottrell, "Deformation of Solids at High Rates of Strain," Report of a Conference on the Properties of Materials at High Rates of Strain, Institution of Mechanical Engineers, (April 1957).

(11) A. H. Cottrell and B. A. Bilby, "Dislocation Theory of Yielding and Strain Aging of Iron", Proceedings, Physical Society of London, (1949), Sec. A, Vol. 62, Part 1, p. 49.

(12) F. C. Frank and W. T. Read, "Multiplication Processes for Slow Moving Dislocations", Physical Review, (1950), Vol. 79, p. 722.

(13) A. H. Cottrell, "The Yield Point in Single Crystal and Polycrystalline Metals", A Symposium on the Plastic Deformation of Crystalline Solids, Mellon Institute, (May 1950), p. 60.

(14) N. J. Petch, "The Cleavage Strength of Polycrystals", Journal of the Iron and Steel Institute, (1953), Vol. 174, p. 25.

(15) E. O. Hall, "The Deformation and Aging of Mild Steel: III", Proceedings of the Physical Society, (1951), Series B, Vol. 64, p. 747.

(16) J. R. Low, Jr., "The Relation of Microstructure to Brittle Fracture", Relation of Properties to Microstructure, American Society of Metals, (1954), p. 163.

REFERENCES (Cont'd)

(17) J. C. Fisher, E. W. Hart, and R. H. Pry, "Theory of Slip-Band Formation", Physical Review, (1952), Vol. 87, p. 958.

(18) T. L. Russell, D. S. Wood, and D. S. Clark, "The Design and Construction of Equipment for Rapid Load Testing", First Interim Technical Report under Office of Ordnance Research, Contract DA-04-495-Ord-171, California Institute of Technology, (March 1955).

(19) D. S. Clark and D. S. Wood, "The Delay Time for the Initiation of Plastic Deformation at Rapidly Applied Constant Stress", Proceedings American Society for Testing Materials, (1949), Vol. 49, P. 717.

(20) J. D. Eshelby, F. C. Frank, and F. R. N. Nabano, "Equilibrium Arrays of Dislocations", Philosophical Magazine, (1951), Vol. 42, p. 351.

(21) J. Frankel, "Zur Theorie der Elastizitätsgrenze und der Festigkeit kristallinischer Körper.", Zeitschrift für Physik (1926), Vol. 37, p. 572.

(22) G. W. Sears and S. S. Brenner, "Metal Whiskers", Metal Progress, (1956), Vol. 70, p. 85.

(23) A. H. Cottrell, Dislocations and Plastic Flow in Crystals, Oxford at the Clarendon Press, (1953).

(24) J. J. Cox, G. T. Horne, R. F. Mehl, "Slip, Twinning and Fracture in Single Crystals of Iron", Transactions of the American Society for Metals, (1957), Vol. 49, p. 118.

(25) A. H. Cottrell and B. A. Bilby, "A Mechanism for the Growth of Deformation Twins in Crystals", Philosophical Magazine, Vol. 42, p. 573.

REFERENCES (Cont'd)

(26) F. C. Hull and W. J. Houk, "Statistical Grain Structure Studies: Plane Distribution Curves of Regular Polyhedrons", Journal of Metals, Metals Transactions, (1953), Vol. 5, p. 565.

(27) E. Scheil, "Statistische Gefugeuntersuchungen I" Zeitschrift für Metallkunde (1936), Vol. 28, p. 340.